JOURNAL OF GEOPHYSICAL RESEARCH, VOL. 107, NO. D15, 4275, 10.1029/2001JD000982, 2002

Background ozone over the United States in summer: Origin, trend, and contribution to pollution episodes

Arlene M. Fiore, Daniel J. Jacob, Isabelle Bey,[1] Robert M. Yantosca, Brendan D. Field, and Andrew C. Fusco

Department of Earth and Planetary Sciences and Division of Engineering and Applied Sciences, Harvard University, Cambridge, Massachusetts, USA

James G. Wilkinson

School of Civil and Environmental Engineering, Georgia Institute of Technology, Atlanta, Georgia, USA

Received 25 June 2001; revised 11 February 2002; accepted 15 February 2002; published 15 August 2002.

[1] Observations indicate that ozone (O_3) concentrations in surface air over the United States in summer contain a 20–45 ppbv background contribution, presumably reflecting transport from outside the North American boundary layer. We use a three-dimensional global model of tropospheric chemistry driven by assimilated meteorological observations to investigate the origin of this background and to quantify its contribution to total surface O_3 on both average and highly polluted summer days. The model simulation is evaluated with a suite of surface and aircraft observations over the United States from the summer of 1995. The model reproduces the principal features in the observed distributions of O_3 and its precursors, including frequency distributions of O_3 concentrations and the development of regional high-O_3 episodes in the eastern United States. Comparison of simulations with 1995 versus 1980 global fossil fuel emissions indicates that the model captures the previously observed decrease in the high end of the O_3 probability distribution in surface air over the United States (reflecting reduction of domestic hydrocarbon emissions) and the increase in the low end (reflecting, at least in the model, rising Asian emissions). In the model, background O_3 produced outside of the North American boundary layer contributes an average 25–35 ppbv to afternoon O_3 concentrations in surface air in the western United States. and 15–30 ppbv in the eastern United States during the summer of 1995. This background generally decays to below 15 ppbv during the stagnation conditions conducive to exceedances of the 8-hour 0.08 ppmv (80 ppbv) National Ambient Air Quality Standard (NAAQS) for O_3. A high background contribution of 25–40 ppbv is found during 9% of these exceedances, reflecting convective mixing of free tropospheric O_3 from aloft, followed by rapid production within the U.S. boundary layer. Anthropogenic emissions in Asia and Europe are found to increase afternoon O_3 concentrations in surface air over the United States by typically 4–7 ppbv, under both average and highly polluted conditions. This enhancement is particularly large (up to 14 ppbv) for O_3 concentrations in the 50–70 ppbv range, and would represent a major concern if the NAAQS were to be tightened. *INDEX TERMS:* 0345 Atmospheric Composition and Structure: Pollution—urban and regional (0305); 0368 Atmospheric Composition and Structure: Troposphere—constituent transport and chemistry; 0365 Atmospheric Composition and Structure: Troposphere—composition and chemistry; *KEYWORDS:* background ozone, ozone pollution, global model, pollution episodes, surface ozone, ozone trends

1. Introduction

[2] Many regions of the United States are plagued by chronic high summertime ozone (O_3) levels produced from rapid photochemical oxidation of carbon monoxide (CO) and hydrocarbons in the presence of nitrogen oxides (NO_x = NO + NO_2) [*National Research Council*, 1991]. In an effort to better protect public health and vegetation from the adverse effects of O_3 pollution, the Environmental Protection Agency (EPA) revised its standard for O_3 in 1997 to a 0.08 ppmv (80 ppbv) annual fourth-highest daily maximum 8-hour concentration averaged over three years [*Environmental Protection Agency*, 2000]. Implementation of this new standard will pose a substantial challenge to the design of effective air pollution control strategies [*Lefohn et al.*,

[1]Now at Swiss Federal Institute of Technology, Lausanne, Switzerland.

0148-0227/02/2001JD000982

Table 1. Summer 1995 Observations Used in This Work

Data Source	Location of Measurements	Sampling Platform	Species	General References
Southern Oxidant Study Nashville/ Middle Tennessee Ozone Study (SOS)	southeastern United States, centered at Nashville	surface	O_3, NO, NO_2, NO_y, PANs,[a] CO, NMHCs[b]	*Meagher et al.* [1998]
		aircraft	O_3, NO, PANs, CO, NMHCs, H_2O_2, CH_2O	*Hubler et al.* [1998] *McKeen et al.* [2001]
North American Research Strategy for Tropospheric Ozone (NARSTO-NE)	northeastern United States	aircraft	O_3, NO, NO_y, CO	*Korc et al.* [1996] *Ryan et al.* [1998]
Harvard Forest	central Massachusetts (43°N, 72°W)	surface	O_3, NO, NO_2, NO_y, CO	*Munger et al.* [1996] *Munger et al.* [1998]
Aerometric Information Retrieval System (AIRS)	950 sites in the United States	surface	O_3	*EPA* [2000]
Clean Air Status and Trends Network (CASTNet)	selected sites in western United States	surface	O_3	*Lavery et al.* [2001]

[a] Peroxyacetyl nitrates including PAN, PMN, and PPN.
[b] Speciated hydrocarbons including isoprene.

1998]. *Saylor et al.* [1998] found that 30–50% of rural sites measuring O_3 in the eastern United States exceeded the 80 ppbv standard during 1993–1995, while only 2–12% did not attain compliance with the prior 120 ppbv 1-hour standard. According to the *Environmental Protection Agency* [2001], 123 million Americans lived in regions failing to achieve compliance with the new standard in 1999.

[3] A substantial fraction of O_3 in surface air over the United States in summer, about 20–45 ppbv, appears to represent a background that either subsides or is horizontally advected into the U.S. boundary layer. The background has been estimated from various techniques, including correlations with reactive nitrogen oxides (NO_y = NO_x + HNO_3 + HNO_4 + PAN + PMN + PPN + alkyl nitrates + $2N_2O_5$), measurements at remote surface sites, and analyses of probability distributions of O_3 concentrations, all of which yield similar values [*Trainer et al.*, 1993; *Hirsch et al.*, 1996; *Lin et al.*, 2000]. Some authors have noted a much larger range of hourly average concentrations at sites considered to measure background levels of O_3 [*Altshuller and Lefohn*, 1996; *Lefohn et al.*, 1998, 2001]. A component of the O_3 background is produced from natural precursor sources, which include NO_x emissions from soil and lightning, and hydrocarbon emissions from vegetation. Nineteenth century observations in Europe suggest that the natural O_3 background is only 5–10 ppbv [e.g., *Anfossi et al.*, 1991; *Marenco et al.*, 1994]. Although these measurements are highly uncertain, they support the contention that present-day background O_3 in Europe as well as in the United States includes an anthropogenic enhancement [*Beck and Grennfelt*, 1994; *Marenco et al.*, 1994; *Kasibhatla et al.*, 1996].

[4] There is limited evidence that background concentrations have risen by a few ppbv in surface air over the United States during the past 2 decades, from observations at Whiteface Mountain, New York [*Oltmans et al.*, 1998], and from an analysis of the probability distribution of daily maximum 8-hour average concentrations at rural sites in the EPA AIRS network [*Lin et al.*, 2000]. Such a rise in the background may thwart efforts to meet the U.S. air quality standard via domestic emission controls, considering the less-than-linear response of O_3 to reductions of anthropogenic NO_x and NMHC emissions [*Liang et al.*, 1998; *Jacob et al.*, 1999; *Sillman*, 1999; *Ryerson et al.*, 2001]. In the coming decades, rising emissions from fossil fuel combustion in developing countries have the potential to further increase this background. As the gap between background O_3 levels and the national air quality standard for O_3 narrows, it becomes increasingly important to understand and quantify the anthropogenic enhancement to the background, since it has the potential to be reduced via international agreements on emission controls [*NARSTO Synthesis Team*, 2000].

[5] In this work, we investigate the origin of the present-day background O_3 in surface air over the continental United States with a three-dimensional global tropospheric chemistry model (GEOS-CHEM) driven by assimilated meteorological data from the Goddard Earth Observing System (GEOS). We focus our analysis on the summer of 1995 because of the wealth of observations of O_3 and related species available from two field campaigns: the North American Research Strategy for Tropospheric Ozone-Northeast (NARSTO-NE) [*Korc et al.*, 1996; *Mueller et al.*, 1996] and the Southern Oxidant Study (SOS) [*Cowling et al.*, 1998, 2000; *Hubler et al.*, 1998; *McNider et al.*, 1998; *Meagher et al.*, 1998]. These campaigns focused on improving the current understanding of regional O_3 pollution over the eastern United States. They allow a regional evaluation of O_3 chemistry in the GEOS-CHEM model, complementing the global evaluations presented elsewhere [*Bey et al.*, 2001a, 2001b; *Li et al.*, 2001; *Liu et al.*, 2001, 2002; *Martin et al.*, 2002; Q. Li et al., Global simulation of tropospheric ozone chemistry over the North Atlantic, 1, Model evaluation and ozone budget, manuscript in preparation, 2002 (hereinafter referred to as Li et al., manuscript in preparation, 2002)]. Another important data set for our work is the ensemble of continuous O_3 observations at 950 surface sites in the United States, compiled by the EPA in the Aerometric Information Retrieval System (AIRS) database. Five major regional episodes of elevated O_3 in the eastern United States in 1995 enable us to examine the background contribution to total surface O_3 over a wide range of conditions.

[6] We provide a summary in section 2 of the meteorological and chemical environment for the summer of 1995. Section 3 presents a brief description of the GEOS-CHEM model as applied to our study. The ability of the model to reproduce the observations from AIRS, SOS, NARSTO-NE, and other programs (Table 1) is examined in section 4.

In sections 5 and 6, we apply the model to investigate the origin of the background O_3 in surface air over the United States via (1) regional source tagging and (2) sensitivity simulations. Conclusions are given in section 7.

2. Meteorological and Chemical Environment for the Summer of 1995

[7] Winds and mixing depths are the critical meteorological variables controlling the dispersion of pollutants and the regional buildup of O_3. The summertime circulation over the United States is governed by the Bermuda and Pacific high pressure systems, as illustrated in Figure 1a with a map of average July 1995 surface winds. Anthropogenic emissions of O_3 precursors in the United States roughly follow population density and are largest in the eastern part of the country and in California. Winds in the southeastern United States are generally weak, promoting the accumulation of pollution. The northeastern United States is usually better ventilated, but weak migratory high-pressure systems episodically traverse the region during summer; the associated high surface temperatures and low wind speeds are conducive to O_3 formation and accumulation [*Logan*, 1989; *NRC*, 1991; *Vukovich*, 1995]. The largest O_3 episode of 1995 occurred in mid-July under these characteristic stagnation conditions. In addition to this major episode, four smaller episodes occurred in the Northeast [*Mueller et al.*, 1996], and one in the Southeast [*McNider et al.*, 1998].

[8] The depth of the mixed layer plays a key role in governing chemical concentrations in surface air. Figure 1b displays the average summer afternoon (1300–1700 local time (LT)) mixing depths from the 3-hour average GEOS data. These mixing depths are diagnosed by the GEOS-1 Data Assimilation System as the pressure level where turbulent kinetic energy is 10% of the surface layer value [*Allen et al.*, 1996]. Typical values are 1–2 km in the eastern United States and 2–4 km in the west (Figure 1b), consistent with the general climatology presented by *Holzworth* [1967], and also with observations from the summer 1995 NARSTO-NE and SOS field campaigns [*Blumenthal et al.*, 1997; *Banta et al.*, 1998; *McNider et al.*, 1998; *Berman et al.*, 1999; *Seaman and Michelson*, 2000]. The latter observations exhibit substantial spatial variations in mixing depth on scales smaller than the $2^\circ \times 2.5^\circ$ GEOS resolution, particularly at coastal locations [*Berman et al.*, 1999] where steep gradients in surface heating exist. The inability of the model to resolve this gradient yields a poor simulation of chemical concentrations at coastal stations, as discussed in section 4.1.

[9] Table 1 lists the observational data sets used to evaluate the GEOS-CHEM simulation over the United States. The AIRS network provides a comprehensive set of data for evaluating the surface O_3 simulation, but aside from California, stations are sparse over the western United States. Figure 2 shows that mean afternoon (1300–1700 LT) O_3 concentrations measured by the AIRS sites during the summer of 1995 are greater than 60 ppbv over large areas of the United States, and exceed 80 ppbv in the Los Angeles area.

[10] The summer 1995 NARSTO-NE and SOS field campaigns provide both aircraft and surface measurements for a variety of species relevant to O_3 production. During the summer of 1995, meteorological conditions conducive to rapid photochemical O_3 production occurred more frequently than would be expected from climatological averages [*McNider et al.*, 1998]. Much work has been done to analyze and model observations from these campaigns [e.g., Southern Oxidants Study Nashville/Middle Tennessee Ozone Study compendium; special section of the Journal of Geophysical Research [April 16, 2000 pp. 9075–9211]); *Anderson et al.*, 1996; *Mueller et al.*, 1996; *Zhang et al.*, 1998; *Ryan et al.*, 1998; *Zhang and Rao*, 1999]. In particular, these studies have examined the chemical and dynamical processes contributing to episodes of regionally elevated O_3 [e.g., *Kasibhatla et al.*, 1998; *McNider et al.*, 1998; *Ryan et al.*, 1998; *Zhang et al.*, 1998; *Seaman and Michelson*, 2000]. The largest exceedances of the national O_3 standard in the eastern United States occurred in mid-July during a classic stagnation event (clear skies, high temperatures, and reduced wind speeds) that ended when a cold front moved through the region [*Mueller et al.*, 1996; *McNider et al.*, 1998; *Olszyna et al.*, 1998; *Seaman and Michelson*, 2000].

[11] An unexpected finding based on the analysis of summer 1995 observations was that Canadian fires in late June and early July produced episodic enhancements of over 100 ppbv to CO levels in the southeastern United States during northerly flow following cold fronts [*Wotawa and Trainer*, 2000]. *McKeen et al.* [2000, 2001] used a regional 3-D photochemical transport model to show that surface O_3 was enhanced by 10–30 ppbv over the eastern United States during the 29 June to 2 July time period when the Canadian fires had their largest impact. They find CO oxidation to be an important source for this O_3 enhancement, particularly over regions with high NO_x emissions where O_3 chemistry is hydrocarbon-limited. Emissions from Canadian forest fires are found to elevate background levels of O_3 over the eastern United States on days when northerly flow would otherwise bring clean air from Canada, but these emissions have little influence on pollution episodes which occur under stagnant meteorological conditions [*McKeen et al.*, 2001].

3. Model Description

[12] The GEOS-CHEM model is a global three-dimensional tropospheric chemistry model driven by assimilated meteorological observations from the Goddard Earth Observing System (GEOS) of the NASA Data Assimilation Office. A detailed description of the model as applied to a global ozone-NO_x-hydrocarbon simulation is given by *Bey et al.* [2001a], and we provide a summary below. The model has previously been applied to a number of tropospheric chemistry problems including ozone over the Pacific [*Bey et al.*, 2001b] and in the Middle East [*Li et al.*, 2001], aerosol tracers [*Liu et al.*, 2001], acetone [*Jacob et al.*, 2002], HCN [*Li et al.*, 2000], and CH_3I [*Bell et al.*, 2002]. Vertical profiles from GEOS-CHEM have been used to constrain retrievals of CH_2O and NO_2 column concentrations from the Global Ozone Monitoring Experiment (GOME) satellite instrument, and the observed columns have been used in turn to evaluate the model [*Palmer et al.*, 2001; *Martin et al.*, 2002, P.I. Palmer et al., Mapping isoprene emissions over North America using formaldehyde column observations

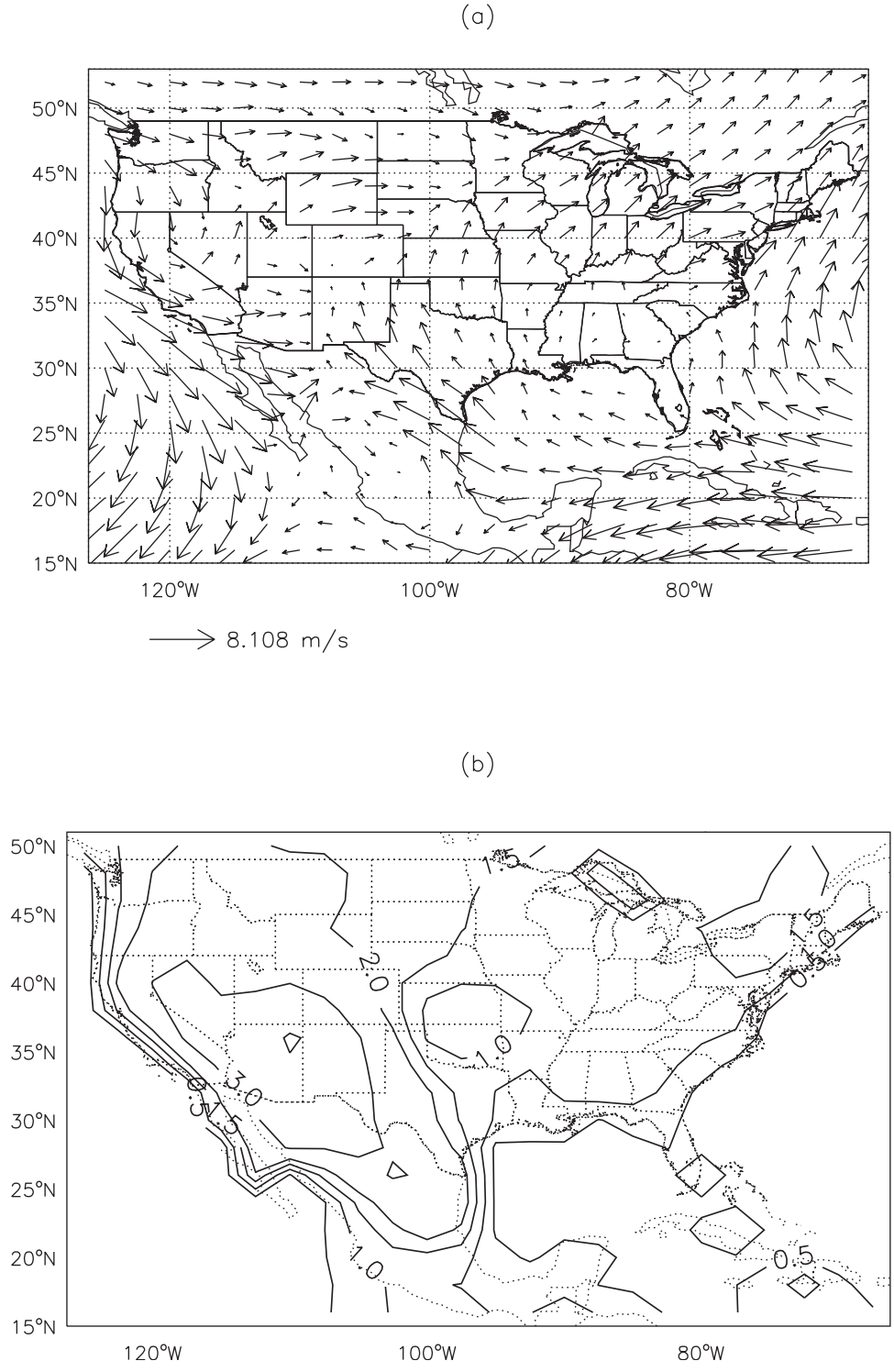

Figure 1. (a) July 1995 mean surface winds over the United States. (b) July 1995 mean afternoon (1300–1700 LT) mixed layer depths (km) over the United States. Data are from the NASA Goddard Earth Observing System (GEOS) assimilation.

from space, submitted to *Journal of Geophysical Research*, 2002 (hereinafter referred to as Palmer et al., submitted manuscript, 2002)].

[13] Several improvements targeted at the present study have been made to the original *Bey et al.* [2001a] version of GEOS-CHEM, as described below. They include (1) inventories for anthropogenic emissions and Canadian forest fires specific to the summer of 1995, (2) accounting for aerosol scattering and absorption of UV radiation in the U.S. boundary layer, and (3) minor updates to the chemical

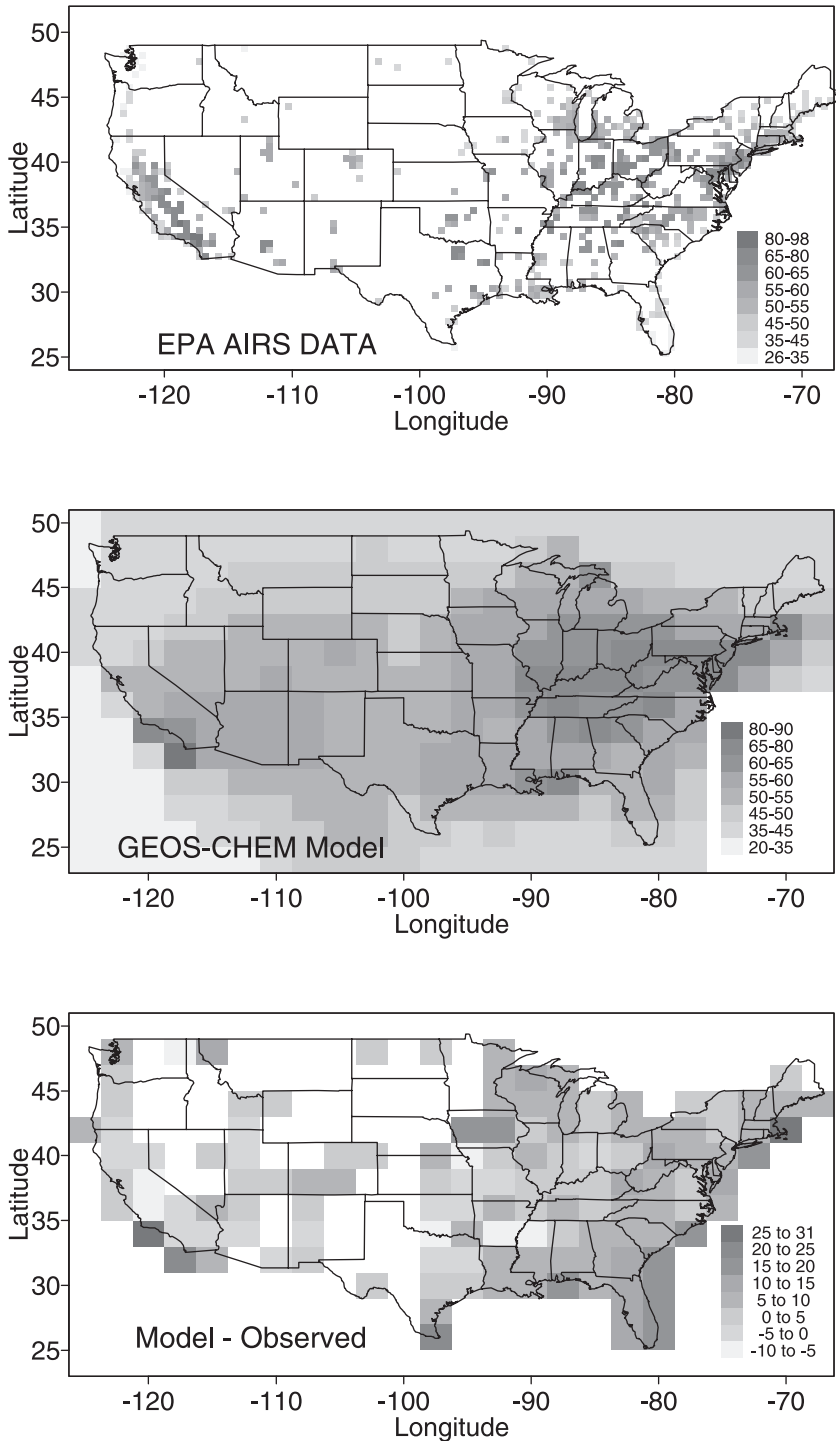

Figure 2. Average afternoon (1300–1700 LT) O_3 concentrations (ppbv) in surface air over the United States in June–August 1995 showing (top) the AIRS observations averaged over a 0.5° latitude by 0.5° longitude grid, (middle) results from the GEOS–CHEM model (2° × 2.5° resolution), sampled in the lowest model layer (0–100 m), and (bottom) the difference between model results and AIRS observations averaged over the 2° × 2.5° model grid. See color version of this figure at back of this issue.

mechanism, the radiative transfer code, and biogenic emissions.

3.1. General Description of GEOS-CHEM

[14] The 1995 GEOS meteorological data used as input to GEOS-CHEM [*Bey et al.*, 2001a] include 3-D fields updated every 6 hours for winds, temperatures, specific humidities, wet convective mass fluxes and detrainment rates, water condensation rates, and cloud optical depths; 2-D fields updated every 6 hours for surface pressures and surface albedos; and 2-D fields updated every 3 hours for column cloud fractions, roughness heights, friction velocities,

Table 2. Anthropogenic Emissions Used for Summer 1995[a]

	Eastern United States (SAMI)	Western United States	Northern Midlatitudes Excluding United States
NO_x (kg N day^{-1})	5.3×10^7	1.1×10^7	9.6×10^7
CO (kg CO day^{-1})	1.5×10^8	6.7×10^7	5.7×10^8
C_2H_6[b]	3.2×10^6	9.7×10^5	6.8×10^6
C_3H_8[b]	3.4×10^6	1.0×10^6	7.6×10^6
$>C_3$ alkanes[b]	1.5×10^7	4.6×10^6	3.1×10^7
acetone	2.3×10^5	1.6×10^5	1.1×10^6
$>C_3$ ketones	8.8×10^4	1.5×10^5	1.1×10^6
$>C_2$ alkenes	3.1×10^6	9.7×10^5	8.9×10^6

[a] Emissions are given in kg C day^{-1} unless stated otherwise. The United States spans 25°N–49°N and 126.25°W–68.75°W, with the east-west division at 98.75°W. The northern midlatitude band encompasses 29°N–61°N, excluding the U.S. domain.
[b] The updated NAPAP inventory is used instead of the SAMI inventory for this species.

surface winds at 10 m altitude, surface temperatures, solar radiation flux at the surface, sensible heat flux, total precipitation at the ground, convective precipitation at the ground, and mixing depths. These data serve as input to different GEOS-CHEM modules that simulate tranport, emissions, photochemistry, and deposition (see Table 1 of *Bey et al.* [2001a] for more information). *Rasch et al.* [1997] have previously shown that the temporal resolution used for the meteorological fields is adequate for the scales of interest in our simulation. The GEOS data are provided on a 2° latitude by 2.5° longitude (2° × 2.5°) horizontal grid with 20 vertical sigma layers, including five located below 2 km altitude (for a column based at sea level, these levels are centered at 50, 250, 600, 1100, and 1750 m). We use this resolution in our standard simulation. A faster version of the model [*Bey et al.*, 2001a, 2001b] uses a 4° × 5° resolution, with GEOS fields regridded accordingly. We conduct our spin-up and sensitivity simulations at this coarser resolution, which is compared with the finer resolved version in section 4. Initial conditions for January 1995 are taken from *Bey et al.* [2001a, 2001b], who had previously run the model from July 1993 through December 1994. We continue to spin up the model until June 1995, and present results from June through August 1995.

[15] Transport of O_3 from the stratosphere is simulated with the Synoz (synthetic ozone) method of *McLinden et al.* [2000] to yield a cross-tropopause flux of 475 Tg O_3 yr^{-1}. Dry deposition velocities are calculated with a resistance-in-series model [*Wesely*, 1989]. The wet deposition scheme is that developed by *Liu et al.* [2001] and is applied here to the soluble gases HNO_3 and H_2O_2.

3.2. Chemical Mechanism

[16] The chemical mechanism is based upon that of *Horowitz et al.* [1998], with modifications by *Bey et al.* [2001a]. It includes 150 reactions among 80 species and integrates the chemical mass balance equations with a fast Gear solver [*Jacobson and Turco*, 1994]. Twenty-four chemical tracers are transported in the model: NO_x ($NO_x = NO_2 + NO + NO_3 + HNO_2$), HNO_3, HNO_4, N_2O_5, O_x ($O_x = O_3 + NO_2 + 2NO_3$), H_2O_2, methyl hydroperoxide, peroxyacetyl nitrate (PAN), peroxymethacryloyl nitrate (PMN), lumped other peroxyacetyl nitrates (PPN), lumped alkyl nitrates, carbon monoxide, ethane, propane, alkanes, alkenes, isoprene, methylvinylketone, methacrolein, acetone, ketones, formaldehyde, acetaldehyde, and lumped other aldehydes. Heterogeneous reactions on aerosols of HO_2 ($\gamma = 0.2$), NO_2 ($\gamma = 10^{-4}$), NO_3 ($\gamma = 10^{-3}$), N_2O_5, ($\gamma = 0.1$) are included [*Jacob*, 2000], with aerosol surface areas from *Chin et al.* [1996] as described by *Wang et al.* [1998a]. We have reduced the yield of isoprene nitrates (products of isoprene oxidation in the presence of NO_x) from the 12% value used by *Horowitz et al.* [1998] and *Bey et al.* [2001a] to the 4.4% value recommended by *Chen et al.* [1998].

3.3. Emissions

3.3.1. Anthropogenic

[17] Global anthropogenic emissions based upon 1985 inventories of NO_x [*Benkovitz et al.*, 1996], nonmethane hydrocarbons [*Piccot et al.*, 1992] and CO [*Wang et al.*, 1998a] are scaled to 1995 levels as described by *Bey et al.* [2001a]. A mean diel cycle [*Jacob et al.*, 1993a] is applied to these emissions. For the western states (west of 98.75°W), the NAPAP inventory for 1985 (described by *Wang et al.* [1998a]) is scaled to 1995 levels according to *EPA* [1997]. For the Ozone Transport Assessment Group (OTAG) region in the eastern United States (68.75°W–98.75°W and 25°N–49°N), we have implemented the Southern Appalachian Mountain Initiative (SAMI) emissions inventory for NO_x, CO and hydrocarbons on 11 July 1995 [*E. H. Pechan and Associates*, 1999; *Ogburn et al.*, 2000], and extrapolated these emissions to the rest of the summer. Table 2 gives daily emission totals for the eastern and western United States and for the northern midlatitudes.

3.3.2. Biomass burning

[18] The GEOS-CHEM model includes a climatology of biomass burning emissions [*Wang et al.*, 1998a], to which we have added Canadian forest fires deemed to be responsible for episodically elevated CO concentrations observed between 25 June and 10 July 1995 in the southeastern United States during the SOS campaign [*Wotawa and Trainer*, 2000]. We have implemented the CO emissions scenario of *Wotawa and Trainer* [2000], which designates five burning areas in northwest Canada and four emission periods from 17 June 17 to 14 July. Emissions of volatile organic compounds (VOCs) are scaled to the reported CO emissions following *Wang et al.* [1998a]. A NO_x/CO emission ratio of 0.0034 mol/mol is adopted for boreal forest fires [*Jacob et al.*, 1992]. The *Wotawa and Trainer* [2000] inventory contributes 15 of the 31 Tg CO produced by boreal fires (north of 48°N) in the model for June through August 1995. We find in our simulation that emissions from Canadian fires enhance CO by over 100 ppbv and O_3 by 4–8 ppbv in late June and in early July at SOS measurement stations.

3.3.3. Natural

[19] Natural sources of NO_x in GEOS-CHEM include lightning (3 Tg N yr^{-1}) and soil (7 Tg N yr^{-1}) [*Bey et al.*, 2001a]. Isoprene is the dominant biogenic hydrocarbon contributing to O_3 production in the boundary layer in the United States [*Trainer et al.*, 1987; *Goldan et al.*, 2000]. Global emission of isoprene in the model is 400 Tg C yr^{-1}, including 30 Tg C yr^{-1} in the United States [*Bey et al.*, 2001a]. Isoprene is oxidized according to the mechanism of *Horowitz et al.* [1998], with updates by *Bey et al.* [2001a]. We have also added a global biogenic source of 8.4 Tg yr^{-1} CH_2O from oxidation of monoterpenes in order to better match CH_2O observations over the United States [*Palmer et al.*, 2001]. This source is based on the monoterpene global emissions inventory of *Guenther et al.* [1995] (120 Tg C yr^{-1}) and a 0.28 CH_2O molar yield from *Orlando et al.* [2000] for monoterpene oxidation.

3.4. Radiative Transfer

[20] Photolysis rate constants in GEOS-CHEM are calculated with the Fast-J radiative transfer code [*Wild et al.*, 2000], which accounts for Mie scattering by clouds and aerosols. Radiative variables include altitude-dependent cloud optical depths from the GEOS archive [*Bey et al.*, 2001a], ultraviolet surface albedos from the TOMS satellite [*Herman and Celarier*, 1997], climatological O_3 columns from *Logan et al.* [1999], and aerosol scattering as described below.

[21] Recent work by *Kondragunta* [1997], *Dickerson et al.* [1997] and *Park et al.* [2002] suggests that O_3 concentrations in the U.S. boundary layer during pollution episodes are enhanced by aerosol radiative scattering that increases the NO_2 photolysis frequency (JNO_2). The effect on photolysis rates and O_3 will vary with the scattering and absorption properties of the aerosols. Over the eastern United States, aerosol optical depths (AOD) at 380 nm are typically less than 0.6 in summer [*Russell et al.*, 1999], but may exceed two during pollution episodes [*Kondragunta et al.*, 1997; *Park et al.*, 2002]. We compute the local AOD in GEOS-CHEM by using a linear relationship between AOD at 380 nm and surface O_3 (ppbv) observed at a nonurban Maryland site by *Kondragunta* [1997] in the summer of 1995: AOD = max(0, ([O_3] − 62)/30). While this parameterization is crude in that it neglects any explicit dependence of AOD on relative humidity, its impact on our simulation is small, as discussed further below. We include the AOD in the radiative transfer code as a submicron aerosol distributed uniformly over the local mixing depth with a gamma size distribution, a modal diameter of 0.1 μm, and a single scattering albedo of 0.96; these parameters are representative of aerosols over the eastern United States [*Dickerson et al.*, 1997]. The corresponding power law dependence of AOD on wavelength has an inverse exponent of 1.7, consistent with the measurements of *Kondragunta* [1997]. For an extreme pollution event with an AOD of 2.0 distributed in this manner under a clear sky, we find that JNO_2 decreases by up to 20% at the surface and increases by 10–30% in the upper part of the mixed layer, consistent with the findings of *Kondragunta* [1997], *Dickerson et al.* [1997], and *Park et al.* [2002].

[22] In our standard simulation, inclusion of scattering aerosols in the mixed layer decreases monthly mean JNO_2 by up to 15% at the surface, and increases it by up to 10% at higher altitudes. The effect on monthly mean O_3 is less than 0.2 ppbv anywhere. Given this small influence on our O_3 simulation, we did not pursue a more complicated representation of AOD in the model. We conducted a sensitivity simulation with an artificially high AOD of 2 to determine the maximal radiative effect of aerosols on O_3; even then, O_3 in the boundary layer increased by less than 2 ppbv over the northeastern United States. Although the addition of scattering aerosols in the GEOS-CHEM mixed layer had little effect on the surface O_3 simulation, aerosols may have a larger impact on O_3 levels in urban airsheds which are not resolved by the model.

4. Model Evaluation

[23] Detailed evaluation of model results with observations, not only for O_3, but also for its precursors and related species, is critical for assessing the ability of the model to describe the processes controlling O_3 [*Sillman*, 1999]. In this work, we focus our evaluation on the United States in the summer of 1995 to diagnose strengths and weaknesses in the model through comparison with the observations in Table 1. The vertical resolution of the model is too coarse to simulate properly the diurnal variation of surface air concentrations driven by mixed layer growth and decay. We focus our analysis on the afternoon hours (1300–1700 LT) when O_3 concentrations are usually highest and when surface observations are representative of a mixed layer sufficiently deep (>100 m) to be resolved by the model.

[24] We begin with a summary of previous evaluations of GEOS-CHEM at northern midlatitudes. Measurements from surface sites, NASA/GTE aircraft campaigns and ozonesondes have been employed by *Bey et al.* [2001a] to compare GEOS-CHEM simulations with seasonal statistics of O_3 and other chemical species affecting the O_3 budget (NO_x, PAN, HNO_3, CO, hydrocarbons, peroxides, and carbonyls). Simulated monthly mean ozone concentrations are typically within 10 ppbv of measured values throughout the troposphere with no systematic bias. The O_3 seasonal cycle as determined from ozonesonde observations at northern midlatitudes is reproduced, with a slight tendency to underestimate the full amplitude of the observed seasonal variation in the middle and upper troposphere, which may indicate that seasonal variation in cross-tropopause transport is too weak in the model. The model generally captures the observed vertical gradients of O_3 at northern mid and high latitudes. *Bey et al.* [2001a] do not find any systematic bias in simulated NO or PAN concentrations in the northern midlatitudes; monthly mean concentrations for these species are generally within a factor of 2 of aircraft observations. As is typical of global models [e.g., *Hauglustaine et al.*, 1998; *Wang et al.*, 1998b; *Lawrence et al.*, 1999; *Mickley et al.*, 1999], HNO_3 is generally overestimated by a factor of 2–3, possibly due to a combination of inaccurate representation of precipitation scavenging, especially in the upper troposphere, and the absence of any partitioning of HNO_3 into the aerosol phase. The model underestimates CO concentrations at northern midlatitudes by an average of 10–20 ppbv. In a more recent version of the model [*Duncan and Logan*, 2001; B.N. Duncan et al., Interannual and seasonal variability of biomass burning emissions constrained by

Table 3. Spatial Statistics for Mean Summer 1995 Afternoon O_3 in Surface Air Over the United States[a]

Statistic	AIRS[b] Observations 0.5° × 0.5° Resolution	AIRS[b] Observations 2° × 2.5° Resolution	Model 2° × 2.5° Resolution	Model 4° × 5° Resolution	Natural Background[c]	No Anthropogenic Emissions in North America[d]	Anthropogenic Emissions in North America Only[e]
Mean, ppbv	54	51	53	51	25	30	46
Variance, ppbv^2	99	80	72	72	10	12	78
Minimum, ppbv	26	26	32	33	17	20	29
Maximum, ppbv	98	68	84	68	31	37	64
Model bias,[f] ppbv	-	-	+5	+3	-	-	-
r^2 (model versus observed)	-	-	0.44	0.70	-	-	-

[a] All statistics are computed from the mean summer (June–August) afternoon (1300–1700 LT) O_3 concentrations for the ensemble of grid squares in the contiguous United States. All available AIRS data, and all model boxes in the United States are included in the calculations. All sensitivity simulations are conducted at the 4° × 5° resolution.

[b] Observations from the AIRS network of sites (Table 1; Figure 2) averaged over either 0.5° × 0.5° or 2° × 2.5° grid squares.

[c] Sensitivity simulation 1, with all anthropogenic emissions of NO_x, CO and nonmethane hydrocarbons turned off, but with present-day levels of methane; see section 6 for details.

[d] Sensitivity simulation 2, with anthropogenic emissions within North America turned off.

[e] Sensitivity simulation 3, with anthropogenic emissions outside North America turned off.

[f] Average difference between the model and the observations when the observations are averaged over the model grid.

satellite observations, submitted to *Journal of Geophysical Research*, 2002 (hereinafter referred to as Duncan et al., submitted manuscript, 2002)], this flaw has been corrected with an additional source of CO from biogenic methanol and updated estimates of nonmethane hydrocarbon emissions from biofuels, fossil fuels, and biomass burning; the present simulation does not include this update. In addition, *Palmer et al.* [2001, submitted manuscript, 2002] have recently evaluated the GEOS-CHEM simulation over the United States with observations of CH_2O from surface sites and find no systematic bias.

4.1. Surface O_3 Over the United States

[25] Figure 2 compares simulated and observed mean afternoon O_3 concentrations in surface air at AIRS stations for the summer of 1995. For the purpose of model evaluation, the AIRS observations were averaged from a $0.5° \times 0.5°$ grid resolution (top panel) to a $2° \times 2.5°$ grid resolution; the bottom panel of Figure 2 shows the difference (model bias). Table 3 shows that the spatial variance in the mean O_3 field decreases by 20% when the AIRS observations are averaged over the $2° \times 2.5°$ model grid, although the mean concentrations are similar. The maximum concentrations are over Los Angeles, where there is a sharp transition from low O_3 concentrations at clean coastal monitoring stations to highly polluted sites in the Los Angeles basin (upper panel of Figure 2). Averaging over the larger model grid smooths out the gradient in O_3 concentrations, yielding the 30 ppbv decrease in the maximum concentration (Table 3).

[26] The model generally reproduces the mean O_3 concentrations, and about half of the variance in the spatial distribution ($r^2 = 0.44$), consistent with simulations from other current global models of atmospheric chemistry and transport [e.g. *Jacob et al.*, 1993a; *Kasibhatla et al.*, 1996; *Horowitz et al.*, 1998; *Lawrence et al.*, 1999]. An overestimate of O_3 concentrations in the southeastern United States is responsible for much of the 5 ppbv bias (Table 3), which decreases to 3 ppbv ($r^2 = 0.52$) when the southeastern quadrant is removed from the analysis. We show below that the model adequately simulates the photochemical relationship governing production of O_3 from its precursor emissions as evidenced by comparison with observed distributions of precursors, O_3 versus $NO_y - NO_x$ correlations, and the response of O_3 to changes in fossil fuel emissions between 1980 and 1995. In a companion study, Li et al. (manuscript in preparation, 2002) find that GEOS-CHEM reproduces observed relationships between O_3 and its precursors over eastern Canada and the western North Atlantic.

[27] The largest discrepancies between the standard simulation and the observations occur for urban coastal grid boxes where the model values are too high, due to steep subgrid land-to-sea gradients in mixing depth that are not resolved in the model. Ventilation of coastal emissions in the model is restricted by shallow mixing depths imposed by the cold ocean surface. The simulation over California is further compromised by the inability of the model to resolve the complex topography controlling airflow and ventilation in that region.

[28] Compared to our standard $2° \times 2.5°$ resolution model, the $4° \times 5°$ resolution model which is applied to our sensitivity simulations in section 6, shows a smaller bias with the observations (+3 ppbv) and a higher coefficient of determination ($r^2 = 0.70$), but smooths out the highest concentrations (Table 3). *Liang and Jacobson* [2000] previously showed that degrading the resolution of a 3-D model can either increase or decrease O_3 depending on local emissions and the photochemical regime. The apparent improvements in the bias and r^2 in our $4° \times 5°$ model relative to the $2° \times 2.5°$ version stem from smoothing out the data, and do not imply that the $4° \times 5°$ resolution model offers a better simulation.

[29] Figure 3 shows the frequency distribution of summer afternoon O_3 concentrations for three representative $2° \times 2.5°$ grid squares in the United States. Observed frequency distributions were constructed using (1) spatial averages of data for the ensemble of the AIRS sites in the grid square and (2) one selected non-AIRS rural site. The model reproduces the frequency distribution observed over the Grand Canyon. It also simulates the high tail of the distribution in the eastern United States, including events with concentrations in excess of 80 ppbv. The lower tail of the distribution is substantially overestimated in the eastern United States, particularly in the southeastern United States (Figure 3). Low O_3 concentrations observed in the southeastern United States are associated with southerly flow from the Gulf of Mexico and the Caribbean, but in the model this southerly flow carries higher O_3 concentrations due to excessive convection over the Gulf of Mexico and the Caribbean, a weakness in the GEOS-1 data previously identified by *Allen et al.* [1997]. *Li et al.* [2002] have shown that this problem is also responsible for a model overestimate of O_3 concentrations in surface air at Bermuda in July.

[30] The overestimate of the low tail of the frequency distribution in the northeastern United States is less severe than in the southeastern United States and stems from different factors. *Lin et al.* [2000] have previously shown that the background O_3 (diagnosed by correlation with low CO and NO_y measurements) at Harvard Forest corresponds to the 25th percentile of the probability distribution in summer. Points below this background level reflect depletion of O_3 from deposition or titration by NO. Since the AIRS sites are predominantly clustered in urban areas, the low values could be indicative of titration by NO in urban plumes that the model does not resolve. The low tail in the GEOS-CHEM model compares well with the observations at Harvard Forest (squares in the top panel of Figure 3), with the exception of the two lowest points; the lowest occurred during tropical storm activity, while the second lowest was associated with northerly flow from Canada.

4.2. Surface Concentrations of Related Species

[31] Surface observations in 1995 for species other than O_3 are limited. Hourly average concentrations of O_3, NO, NO_y, and CO were recorded at seven surface sites as part of SOS (Table 1) [*Meagher et al.*, 1998; *Olszyna et al.*, 1998]. We sampled the model grid square centered at 36°N and 87.5°W over Tennessee and compared its O_3, NO, NO_y, and CO concentrations with those recorded at two suburban (Youth Incorporated and Dickson County in Tennessee) and two rural (Giles County, Tennessee, and Land Between the Lakes, Kentucky) sites within the grid square. Figure 4 shows the time series of median O_3, NO, NO_y, and CO

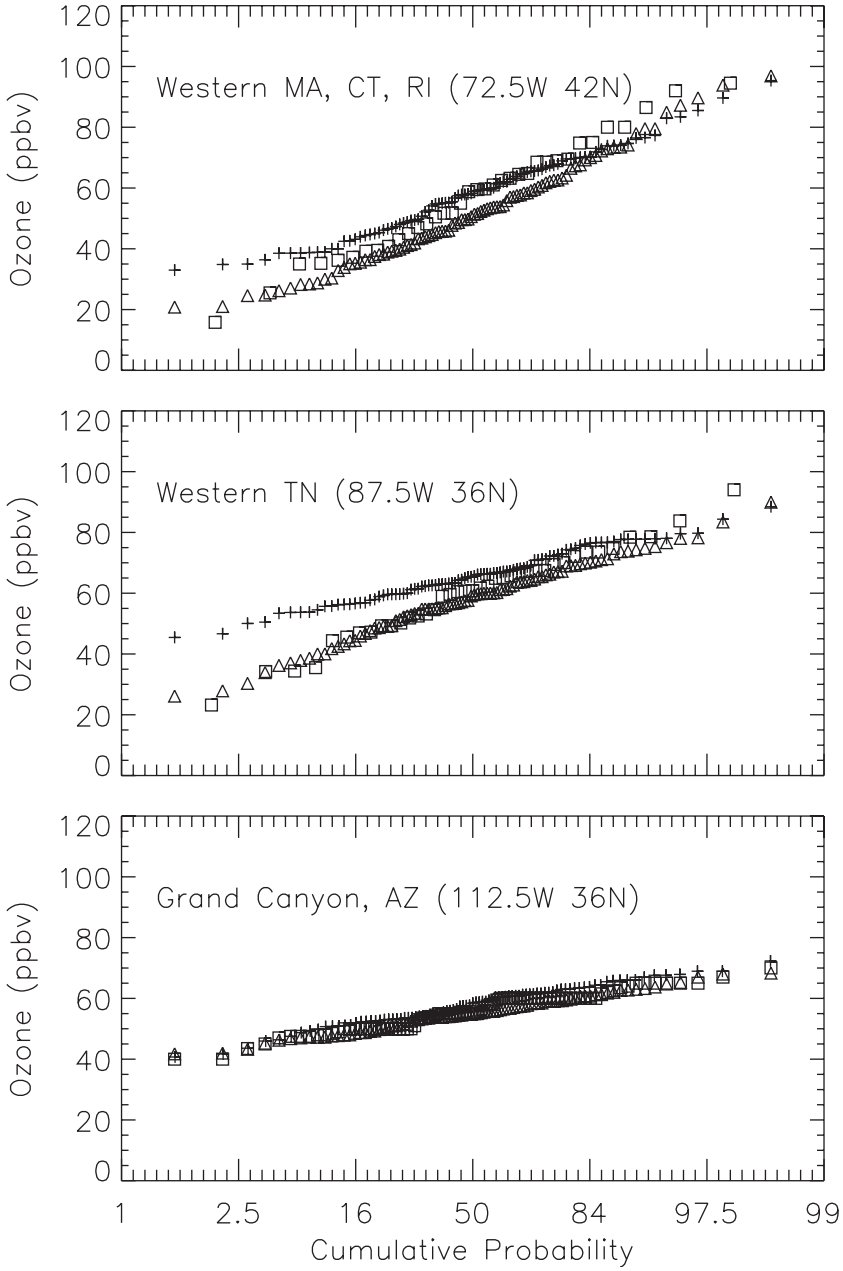

Figure 3. Cumulative probability distributions of mean daily 1300–1700 LT O_3 concentrations in surface air during summer 1995 over 2° × 2.5° grid squares centered at (top) 72.5°W 42°N (western Massachusetts, Connecticut and Rhode Island), (middle) 87.5°W 36°N (western Tennessee), and (bottom) 112.5°W 36°N (northern Arizona). Crosses are GEOS-CHEM model results. Triangles are EPA AIRS data averaged over the 2° × 2.5° resolution of the model. AIRS data are taken from 24–26 sites in western Massachusetts, Connecticut, and Rhode Island, 8–11 sites in western Tennessee, and 1 site in northern Arizona. Squares show the O_3 distribution at selected rural non-AIRS sites in the grid square: Harvard Forest in central Massachusetts, Giles County in Tennessee, and Grand Canyon National Park in Arizona.

observations for the four sites (solid lines) along with the extreme values (dotted lines). Local pollution plumes are responsible for the large envelope between the two extremes, particularly for NO and NO_y.

[32] The modeled time series for NO, NO_y, and O_3 (dashed lines) usually fall within the observed ranges. The model simulates summer afternoon median values of 0.11 ppbv NO and 3.21 ppbv NO_y as compared to the observed 0.10 ppbv NO and 3.8 ppbv NO_y, indicating biases of less than 20%. Poor correlations between the median observed and simulated time series ($r^2 = 0.09$ for NO, and $r^2 = 0.22$ for NO_y) may reflect the influence of subgrid plumes. Summer afternoon median concentrations of O_3 are 65 ppbv in the model and 62 ppbv observed, with an

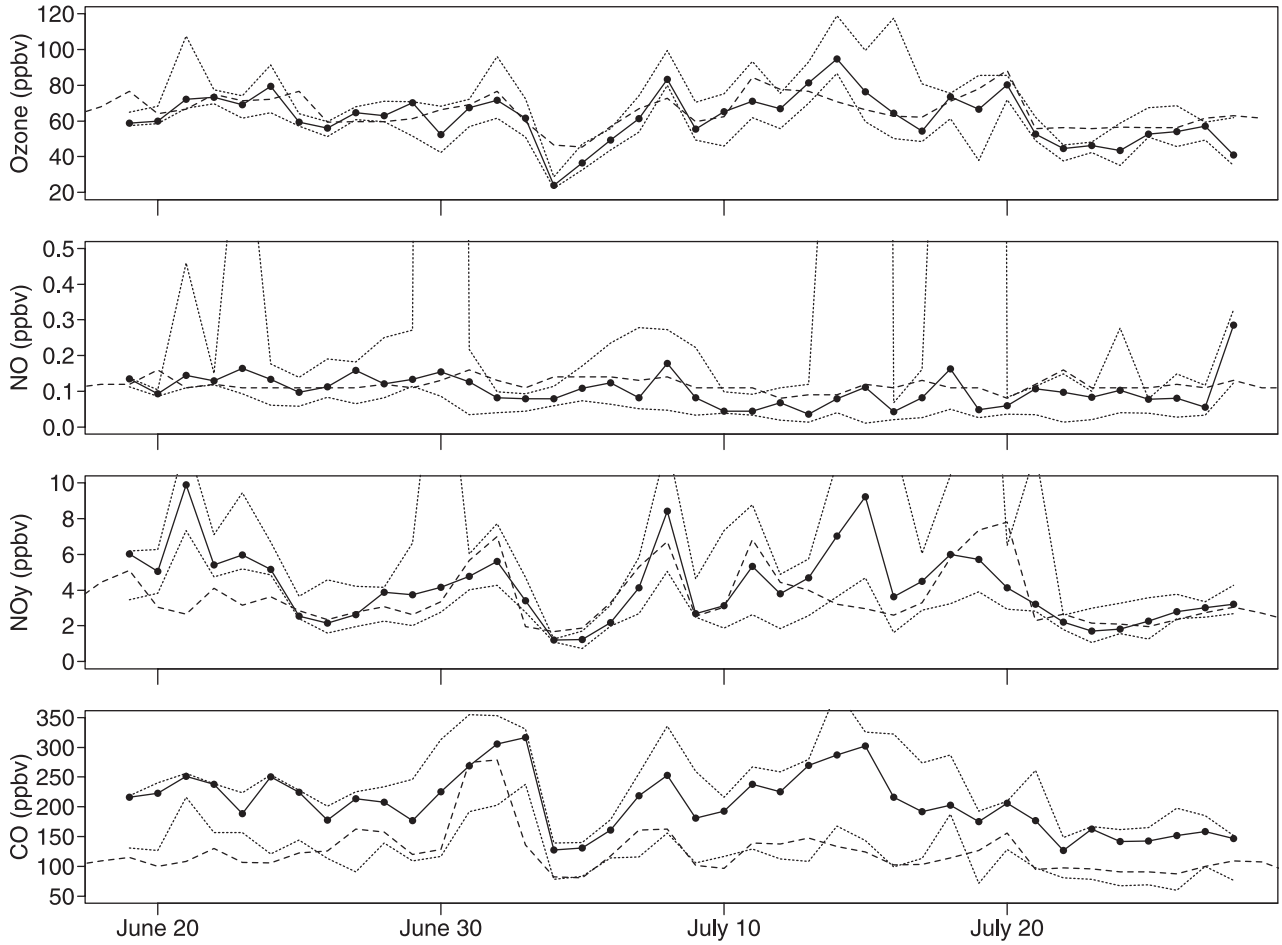

Figure 4. Time series of summer 1995 mean afternoon (1300–1700 LT) O_3, NO, NO_y, and CO concentrations in the Nashville, Tennessee, area. The dashed line is the GEOS-CHEM model sampled in the Nashville grid box centered at 87.5°W 36°N. The solid lines with dots and the dotted lines show the median and ranges of measurements at four suburban and rural stations falling within the grid box (Youth Inc., Giles County and Dickson, Tennessee, and Land Between the Lakes, Kentucky).

r^2 = 0.54 for the time series. The peaks in O_3 and NO_y concentrations during the episode in mid-July (14–15 July) are not captured properly; it rains in the model on these days, unlike in the observations.

[33] Concentrations of CO in the model are severely underestimated, by 100 ppbv or more (summer median is 110 ppbv in the model and 207 ppbv in the observations; r^2 = 0.38), with the exception of early July when the influence of the Canadian fires reaches Tennessee, and the model predicts values consistent with the observations (above 270 ppbv on 1 and 2 July). As discussed previously, missing background sources of CO may improve the model simulation [*Duncan et al.*, 2001; submitted manuscript, 2002] but cannot provide the whole explanation. The model tends to capture CO concentrations at the Dickson County site, where surface measurements of CO were consistently lower than those at the other three sites. While the instrument at Dickson passed QA/QC protocols, aircraft measurements above Dickson are consistent with the observations at the other surface sites, leaving the discrepancy in surface CO concentrations unexplained [*Luke et al.*, 1998].

[34] We conducted a more general evaluation of the model simulation over the United States by comparing the GEOS-CHEM simulation for 1995 with median or mean June–August observations available from earlier years (1975–1995) for a number of species at nonurban U.S. locations, as previously done by *Horowitz et al.* [1998] for evaluating an earlier version of the Harvard model. Results are shown in Figure 5. The locations of the measurement sites, length of data record (the entire set of observations spans 1975–1995), and statistic used in the comparison are listed in Table 3 of *Horowitz et al.* [1998]. Modeled NO_y and NO_x are typically within 50% of the observations, without systematic bias. The model underestimates PAN by 30% on average. The sparsity of data (three sites) prohibits a conclusive discussion of the HNO_3 simulation. From the three available measurements, the model appears to overestimate H_2O_2 by 1 ppbv, perhaps because it does not account for reaction with SO_2 in clouds. Of note, *Bey et al.* [2001a] do not find a global systematic bias in the GEOS-CHEM simulation for H_2O_2. The most striking feature in the comparison is the underestimate of CO, with an average bias of 60 ppbv. In addition to the factors

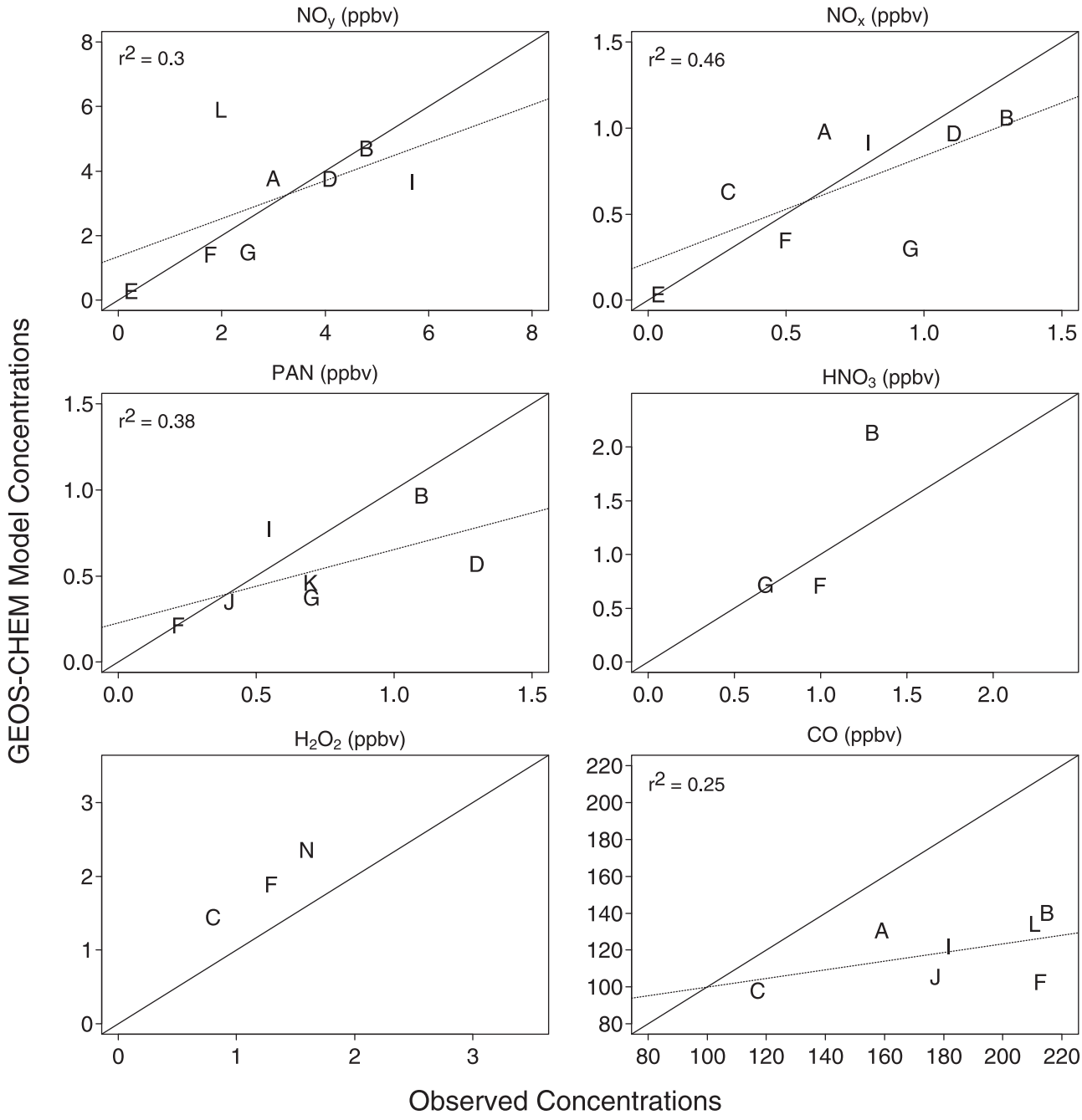

Figure 5. Correlation between simulated and observed summer median or mean afternoon concentrations at nonurban sites [*Horowitz et al.*, 1998]. Model results are for 1995 while observations are from different years in the 1975–1995 window. Letters represent specific sites: A. Harvard Forest, Massachusetts (43°N, 72°W); B. Scotia, Pennsylvania (41°N, 78°W); C. Niwot Ridge, Colorado (40°N, 105°W); D. Bondville, Illinois (40°N, 88°W); E. Schefferville, Quebec (55°N, 67°W); F. Metter, Georgia (33°N, 82°W); G. Egbert, Ontario (44°N, 80°W); I. Central Piedmont, North Carolina (35°N, 80°W); J. Pride, Louisiana (31°N, 91°W); K. Elberton, Georgia (34°N, 83°W); L. Shenandoah National Park, Virginia (39°N, 79°W). Details and references for the concentration statistics used for each site are given in Table 3 of *Horowitz et al.* [1998]. The solid line is $y = x$. The dashed line is the linear regression.

discussed previously, part of the discrepancy may stem from declining CO emissions in the United States in the late 1980s and the 1990s, as evidenced by decreasing CO concentrations [*Hallock-Waters et al.*, 1999; *Parrish et al.*, 2002].

[35] We investigated the ability of the model to reproduce the O_3:[$NO_y - NO_x$] correlations observed at nonurban sites. The intercept of the regression line from this correlation indicates the background O_3 concentration, while the slope is an upper limit estimate of the O_3

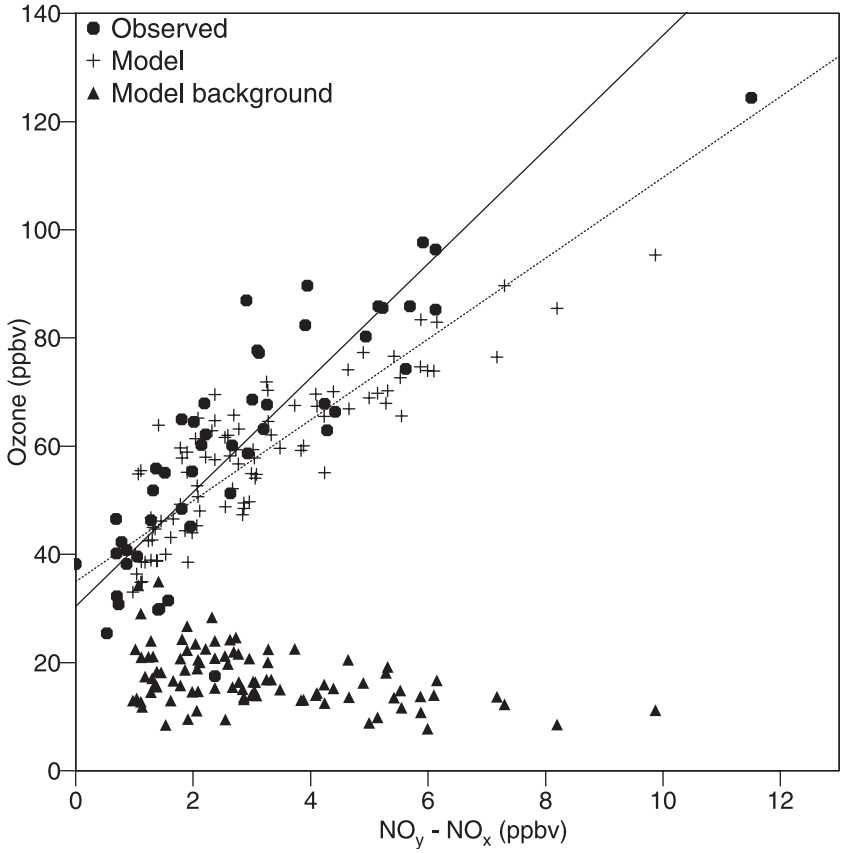

Figure 6. Correlation of afternoon (1300–1700 LT) O_3 and $NO_y - NO_x$ concentrations at Harvard Forest, a rural site in central Massachusetts, for the summer of 1995. Observations are depicted as circles. Model results are shown as crosses. The reduced major axis method is used to calculate the regression line [*Hirsch and Gilroy*, 1984]. Background O_3 originating outside the North American boundary layer in the model is shown as triangles (see section 5 for details).

production efficiency (number of O_3 molecules produced per molecule of NO_x oxidized) [*Trainer et al.*, 1993; *Olszyna et al.*, 1994; *Hirsch et al.*, 1996; *St. John et al.*, 1998; *Sillman*, 1999]. Figure 6 shows the comparison with summer 1995 observations at Harvard Forest. The slope of the regression line is 7.5 mol/mol in the model and 10.6 mol/mol in the observations; the intercept (background O_3) is 35 ppbv in the model and 30 ppbv in the observations. These values are typical of previous summertime observations at Harvard Forest (8.0 mol/mol slope and 20–40 ppbv intercept) [*Hirsch et al.*, 1996], and at Scotia, Pennsylvania (8.5 mol/mol slope and 35 ppbv intercept) [*Trainer et al.*, 1993].

4.3. Aircraft Observations

[36] Two low–flying aircraft were deployed along the northeastern U.S. urban corridor as part of NARSTO-NE. Figure 7 shows measured O_3 distributions (colored lines) during horizontal afternoon transects between 400 and 800 m altitude on a highly polluted day (14 July 1995) and on a relatively clean day (10 August 1995). On 14 July, O_3 levels are well above 80 ppbv over most of the flight track, with a peak of 193 ppbv. Concentrations are below 55 ppbv over much of the region sampled on 10 August, with the largest values recorded over Long Island and southern Connecticut. The model (numbers in boxes) simulates the contrast in O_3 concentrations observed on these two days, but fails to reproduce the levels over 90 ppbv recorded on 14 July. Grid-scale dispersion of emissions prevents the model from capturing the extreme range of O_3 concentrations.

[37] Since subsidence from the free troposphere accounts for a large fraction of background O_3 in surface air, it is critical to inspect the model simulation of the chemical gradients between the boundary layer and the free troposphere. We previously summarized the extensive evaluation of model results with ozonesonde vertical profiles at northern midlatitudes [*Bey et al.*, 2001a]. As part of the SOS campaign, the NOAA WP-3D aircraft flew on eighteen days in the boundary layer and free troposphere over Nashville and the surrounding region, measuring a suite of chemicals [*Hubler et al.*, 1998]. In Figure 8, we show a comparison for three days (26 June, 1 July, and 11 July) that best exemplify the different structures in the vertical distribution of O_3. On both 26 June and 1 July, the aircraft flew over Tennessee and Kentucky, while on 11 July, it headed north into Illinois, Indiana and Ohio. On 26 June, there is little structure in the O_3 profile. Concentrations of O_3 are relatively low in the boundary layer, and higher in the free troposphere where values are typical of the climatology [*Logan*, 1999]. The O_3 profile on 1 July exhibits more structure, with concentrations reaching above 80 ppbv near the surface, and decreasing to below 60 ppbv above the boundary layer. On the 11

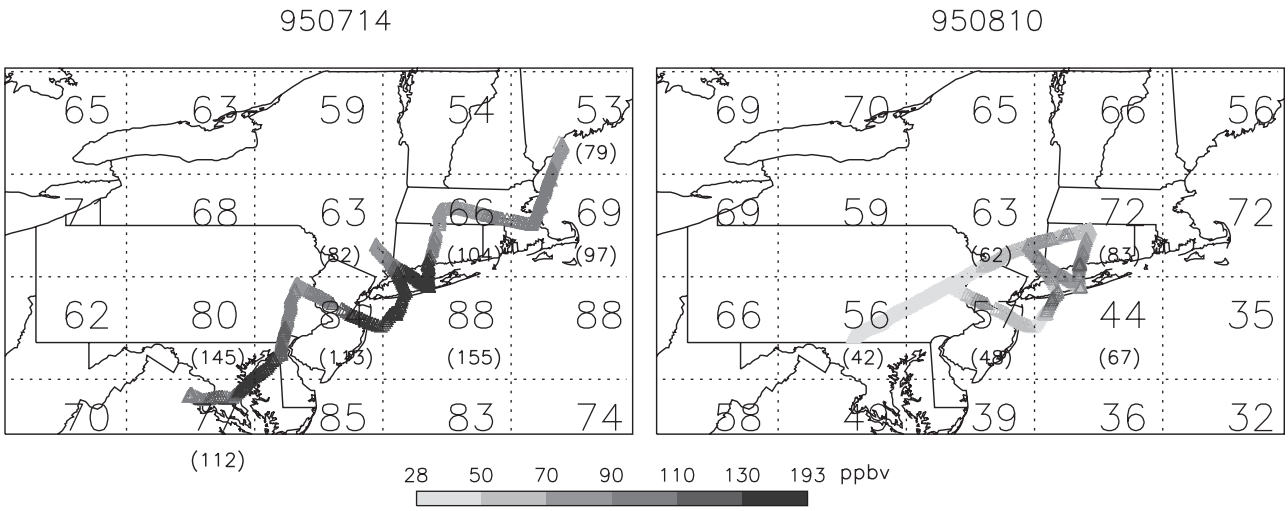

Figure 7. Ozone concentrations (ppbv) at 400–800 m altitude over the northeastern United States on 14 July and 10 August 1995. The lines show observations from the two NARSTO-NE aircraft. The model grid is superposed on each map, with the model O_3 concentration for that day (1300–1700 LT) printed at the center of each model box. Smaller numbers in parentheses are the average of all the aircraft data falling within each model grid box. We have selected days when both NARSTO-NE aircraft flew, providing the largest spatial coverage over the northeast region. See color version of this figure at back of this issue.

July flight, the aircraft sampled surface O_3 concentrations above 100 ppbv. Concentrations decrease sharply upwards from the surface to 2 km, where O_3 levels are below 50 ppbv. The vertical profiles of PAN and CO exhibit similar behavior to those of O_3, with higher surface values measured on 1 July and 11 July. The vertical distributions of NO and CH_2O show a sharp decrease from the boundary layer to the free troposphere without much variation over the three days, although CH_2O concentrations are particularly high in the boundary layer on 11 July in association with the high-O_3 episode. Unlike the other species, H_2O_2 concentrations do not generally decline from the boundary layer to the free troposphere, but instead remain fairly uniform until 4 km, where they begin to decrease.

[38] The model captures much of the spread in the surface observations of O_3, CH_2O, and H_2O_2, along with the day-to-day variability in the observed vertical distribution of O_3. The overestimate of O_3 between 2 and 6 km apparent on 1 July and 11 July does not appear to be systematic when observations from the additional flight days are considered; the observations are particularly low above 1 km on 11 July. High CO concentrations simulated on 1 July are due to Canadian fire plumes [*Wotawa and Trainer*, 2000]. At the surface, peak values of NO, CH_2O and PAN are sometimes underestimated. These measurements were most likely influenced by the Nashville plume or the plumes of neighboring power plants not resolved in the model. Above the surface, CH_2O appears to be underestimated between 2 and 4 km on 1 July and 11 July. When we consider the entire SOS 1995 set of CH_2O aircraft data, we find that on average, the model underestimates CH_2O concentrations by 0.5–1 ppbv on average at all altitudes. The model shows a tendency to underestimate H_2O_2 between 2 and 6 km, although it reproduces the surface concentrations fairly well. This result contradicts the surface overestimate in H_2O_2 in the southeastern region noted in section 4.2 (at Metter, Georgia, and Kinterbish, Alabama).

4.4. Response of Surface O_3 to Anthropogenic Emission Changes From 1980 to 1995

[39] We conduct a simulation with 1980 levels of fossil fuel emissions in order to test that the model adequately captures the trends that have been reported in previous analyses of surface O_3 measurements over the United States from 1980 to 1995 by *Lefohn et al.* [1998] and *Lin et al.* [2000]. We examine differences in the O_3 simulation for the month of July in the $2^\circ \times 2.5^\circ$ resolution model, after a full year of spin-up with 1980 emissions at $4^\circ \times 5^\circ$ resolution. Any change in the O_3 simulation is fully attributable to the differences in fossil fuel emissions from 1980 to 1995 since all other parameters (e.g., meteorology, all other emissions) were held constant. Global anthropogenic emissions of NO_x, CO, and nonmethane hydrocarbons for 1980 are implemented into the model by applying scaling factors (described previously in section 3.3) uniformly to individual nations; changes in CH_4 concentrations are not considered. Global NO_x emissions from fossil fuel increased by 20% from 1980 to 1995, primarily due to a doubling of emissions from Asia (emissions increased by 2% over North America and decreased by 13% over Europe). Global fossil fuel emissions of CO and nonmethane hydrocarbons exhibited little change during this time period, with emission controls in Europe (35% decrease) and North America (15% decrease) offset by rising Asian emissions.

[40] Previous analyses of surface O_3 measurements have shown that the highest levels of O_3 exhibited the largest decreases in response to the reductions in hydrocarbon emissions during 1980-1995. *Lefohn et al.* [1998] observed what they called a "piston effect": midlevel (60–90 ppbv) O_3 concentrations at AIRS and CASTNET sites decreased

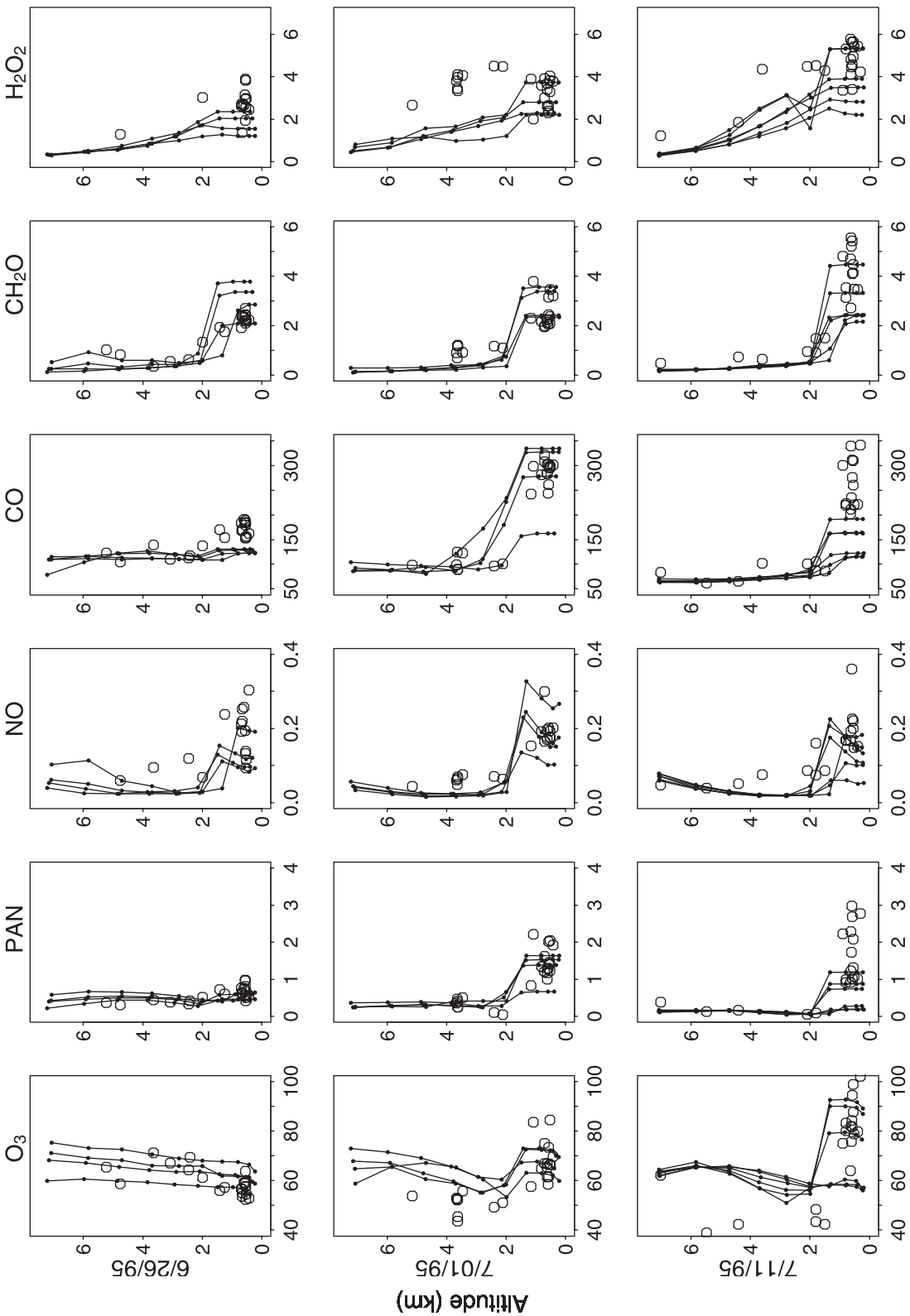

Figure 8. Observations from SOS (open circles) and average 1300–1700 LT GEOS-CHEM vertical profiles (lines) for O_3, precursors and related species on 26 June, 1 July, and 11 July 1995 over the Nashville region. The lines correspond to the simulated profiles over the range of grid squares sampled by the aircraft for each particular day.

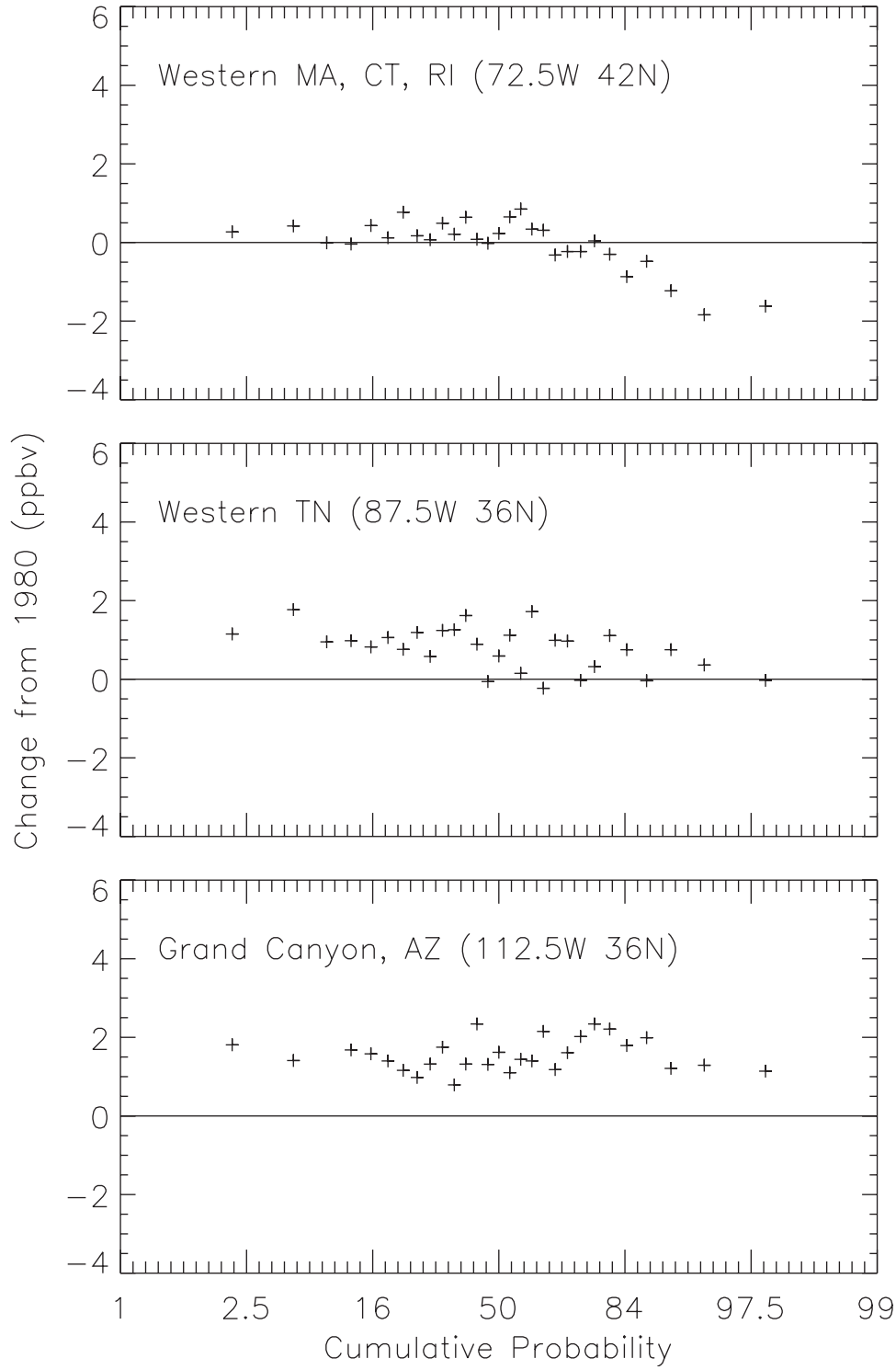

Figure 9. Change from July 1980 to July 1995 in mean daily 1300–1700 LT O_3 concentrations in the GEOS-CHEM surface layer, plotted as a function of the cumulative probability distributions shown in Figure 3. The solid line denotes zero change from 1980; the crosses represent the difference between the 1995 and the 1980 simulations. The 2° × 2.5° grid squares are centered at 72.5°W 42°N (western Massachusetts, Connecticut, and Rhode Island), 87.5°W 36°N (western Tennessee), and 112.5°W 36°N (northern Arizona). The O_3 distributions at these three locations are shown for the entire summer of 1995 in Figure 3 (crosses).

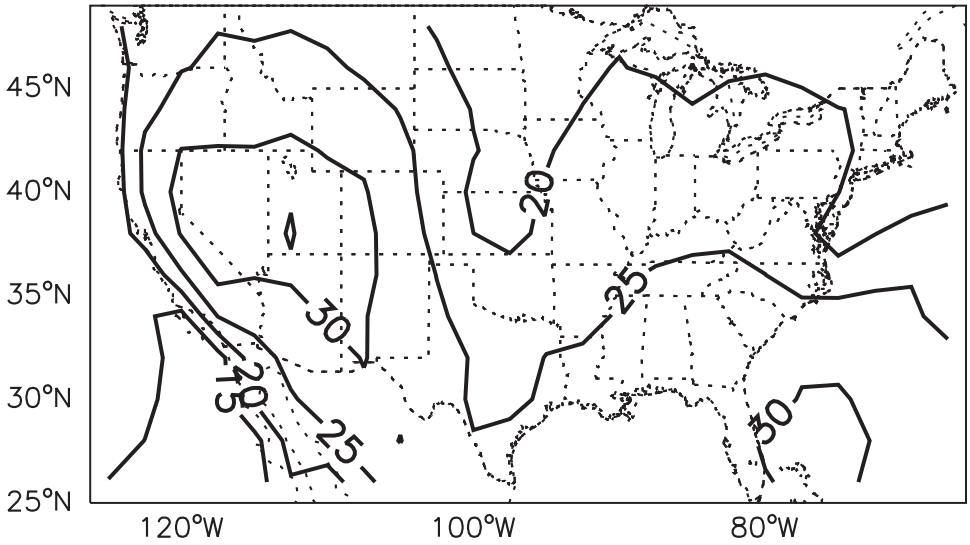

Figure 10. Mean afternoon (1300–1700 LT) background O_3 concentration (ppbv) in surface air in the GEOS-CHEM model for the summer of 1995. The background is defined as O_3 produced outside the North American boundary layer (surface to 700 hPa).

less than the highest O_3 values (above 90 ppbv) from the early 1980s to 1995. In addition, they found a tightening of the overall O_3 distibution due to increases in the lowest concentrations. *Lin et al.* [2000] found similar results in a comparison of probability distributions of daily maximum 8–hour average O_3 concentrations at rural AIRS sites for 1980–1984 versus 1994–1998.

[41] Figure 9 shows the simulated effect on the frequency distributions of July afternoon (1300–1700 LT) O_3 in surface air for the three grid squares discussed in section 4.1. Over western Massachusetts (top panel), we find that the piston effect is qualitatively reproduced, with the highest O_3 values exhibiting the largest response to the reductions in U.S. hydrocarbon emissions between 1980 and 1995. In the lower half of the distribution, O_3 concentrations show a slight increase from 1980, consistent with the observations shown by *Lin et al.* [2000]. The simulated increases over western Tennessee (middle panel) and the Grand Canyon (bottom panel) can be attributed to the global rise in anthropogenic emissions in the model from 1980 to 1995. The enhancement to the background from Asian emissions is explored further in section 6 for the standard 1995 simulation. While the piston effect is not clearly manifested in the model over Tennessee, the highest values increased by smaller amounts as compared to the lower half of the distribution. *Jacob et al.* [1993b] previously showed a greater response of O_3 to hydrocarbon emissions controls in New York and Michigan than in Georgia in their model. They attributed this result to the role of abundant natural isoprene emissions in reducing the sensitivity of O_3 production to changes in anthropogenic hydrocarbon emissions in the southeastern United States.

4.5. Summary of Model Evaluation

[42] Our evaluation of the GEOS-CHEM model over the United States has identified four main problems: (1) excessive convective mixing over the Gulf of Mexico and the Caribbean, (2) poor resolution of the gradient in mixed layer depths between land and sea, (3) an inability to resolve topography over California, and (4) a substantial underestimate of CO concentrations. The first problem leads to an overestimate of background O_3 in surface air in the southeastern United States, while the second compromises the model simulation over coastal urban environments. The third problem is manifested over the Central Valley region of California. The fourth problem is difficult to fully attribute, but should be of little consequence for our study since O_3 production is largely NO_x-limited.

[43] The model generally captures the day-to-day variability in species concentrations, both at the surface and aloft. Episodes of elevated O_3 over the eastern United States are reproduced although peak levels on scales smaller than the $2^\circ \times 2.5^\circ$ model resolution are underestimated (Figure 4). Much of the relevant variance in the O_3 distribution is simulated (Figures 2 and 3), with the exception of the background O_3 problem in the southeastern United States. The simulated O_3:$[NO_y - NO_x]$ relationships, CH_2O concentrations, and response of O_3 to global fossil fuel emission changes from 1980 to 1995 further imply a good simulation of the photochemical environment.

5. Background O_3 Over the United States

[44] We apply the model to quantify the contribution of transport from outside North America to afternoon O_3 concentrations in surface air over the United States. We define North America to be the region north of 13°N, and between 69°W and 126°W. We label, or tag, O_3 in the model by its region of production, as done by *Wang et al.* [1998c]. Tagging O_3 involves archiving 3-D fields of daily mean production and loss frequencies of the extended odd oxygen family ($O_x = O_3 + O + NO_2 + 2NO_3 + PANs + HNO_4 + HNO_3 + 3N_2O_5$) from our standard simulation. O_x will be hereafter referred to as O_3 since O_3 usually accounts for over 95% of O_x. The archived production and loss frequencies are used to drive an off-line simulation, in which total

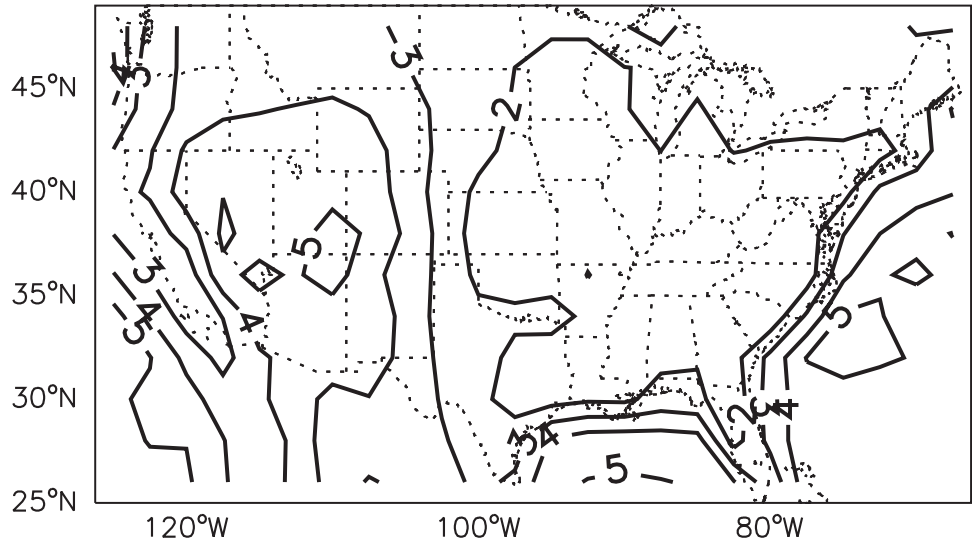

Figure 11. Mean lifetime (days) of O_3 (actually the extended O_x family; see text) in the mixed layer over the United States in summer, as calculated with the model from 24-hour average O_3 concentrations, deposition velocities, and chemical loss rates summed over the local afternoon (1300–1700 LT) mixed layer depth (Figure 1b).

O_3 is divided into individual tagged tracers produced in different regions of the atmosphere. Each tracer is subjected to the same chemical loss and dry deposition frequencies as the total O_3, but is produced only within its specific source region. This approach allows surface O_3 over the United States to be deconstructed into two separate components: (1) O_3 produced inside the North American boundary layer (defined as extending up to 3 km altitude or ~700 hPa) and (2) the O_3 background (produced outside). The O_3 background is further decomposed into contributions from tropospheric production and stratospheric injection.

[45] Five months of initialization (January–May 1995) were found appropriate for the tagged tracer model. After this time the initial conditions contribute only a few percent to the total O_3. The sum of O_3 from all source regions is within a few percent of the total O_3 in the standard full-chemistry simulation.

[46] Production in the North American boundary layer is found to account for 50% of surface afternoon (1300–1700 LT) O_3 concentrations over the United States in summer, and the remainder is mainly from tropospheric production outside the region. We find that stratospheric injection of O_3 never contributes more than 2 ppbv to these concentrations. This result is consistent with that of *Follows and Austin* [1992], who showed that O_3 originating in the stratosphere composes less than 5% of zonally averaged O_3 near the surface.

[47] Figure 10 shows the mean summer afternoon (1300–1700 LT) background O_3 concentration in the model surface layer. Average background concentrations are 15–35 ppbv, with highest values in the west. The larger background in the west reflects the arid climate with its deep boundary layer mixing, slow deposition velocities, and long O_3 lifetime.

[48] Indeed, the lifetime of O_3 in the U.S. boundary layer is critical for understanding the magnitude of the background. The mean lifetime of O_3 in the GEOS-CHEM mixed layer in summer is displayed in Figure 11. This lifetime is calculated from 24-hour average O_3 concentrations, deposition velocities, and O_x chemical loss rates summed over the local afternoon (1300–1700 LT) mixed layer depth (Figure 1b). The afternoon mixed layer is assumed to represent the depth of the planetary boundary layer that is in daily contact with the surface. In the western states, the chemical lifetime for O_3 in the mixed layer is as long as 10 days, while the lifetime against dry deposition is about 6 days (mixing depths are about 2 km on average, with average deposition velocities of 0.4 cm s^{-1}), yielding an O_3 lifetime of 3–5 days (Figure 11). The lifetime in the eastern states is typically less than 2 days, reflecting shallow mixing depths (1 km on average), faster deposition velocities (0.5 cm s^{-1} on average), and more active chemical loss. The short chemical lifetime of O_3 in the east is due in part to reactions with biogenic hydrocarbons. Table 4 quantifies the relative importance of various loss pathways for O_3 in the mixed layer for different regions. Reaction of O_3 with biogenic hydrocarbons contributes 10–20% to O_3 loss in the eastern United States while deposition of HNO_3 contributes 5–10%. Aqueous reaction with SO_2 in clouds is a negligible sink for O_3 [*Jacob*, 2000].

[49] The short lifetime of O_3 in the mixed layer over the eastern United States effectively reduces the contribution of the background during episodic pollution events associated with stagnation and strong subsidence inversions. To illustrate this point, we show in Figure 6 (triangles) the simulated afternoon background at Harvard Forest, as a function of ($NO_y - NO_x$), which serves here as an index of aged pollution. The background decreases with increasing ($NO_y - NO_x$), and drops below 12 ppbv at the highest O_3 concentrations. Figure 6 indicates that inferring a background contribution to episodes of elevated O_3 from either average conditions or from the intercept of an O_3:($NO_y - NO_x$) correlation plot leads to a substantial overestimate of

Table 4. Pathways for Ozone Loss in the U.S. Mixed Layer[a]

Loss Pathway[b]	Percentage (%) of Total O_x Lost Via This Pathway		
	Western United States	Northeastern United States	Southeastern United States
Deposition of O_3	55–95	30–60	30–50
$O^1D + H_2O$	1–15	15–30	15–45
$O_3 + HO_x$	0–15	10–25	10–15
O_3 + biogenic hydrocarbons	1–5	5–15	15–20
Deposition of HNO_3[c]	2–10	5–10	5–10
Deposition of NO_2	0–2	0–2	0–1

[a] Ozone is defined here as odd oxygen ($O_x = O_3 + O + NO_2 + 2NO_3 + PANs + HNO_4 + HNO_3 + 3N_2O_5$). The mixed layer is the mean summertime local afternoon (1300–1700 LT) mixing depth shown in Figure 1b. The Western United States spans from 97.5°W–122.5°W and 32°N–48°N; Northeastern United States extends from 72.5°W–97.5°W and 36°N–48°N; Southeastern United States encompasses 77.5°W–97.5°W and 28°N–36°N. Oceanic regions are excluded.

[b] Other loss pathways that do not contribute more than 1% anywhere within the U.S. domain include NO_3 reactions, heterogeneous loss of NO_2 on aerosols, thermal decomposition of PAN to methyl nitrate and CO_2, and deposition of PAN species.

[c] Includes wet and dry deposition.

the role of the background on highly polluted days in the eastern United States.

[50] Our general finding that background O_3 is low during high-O_3 episodes leads us to examine whether the background is ever substantial on days when O_3 is elevated above 80 ppbv. Figure 12 presents the probability distribution of afternoon background O_3 concentrations in the model surface layer for two populations: (1) the ensemble of summer afternoon 1995 data in the United States and (2) the data subset in which total afternoon surface O_3 was above 80 ppbv (dashed line). The mode for the full summer 1995 data set is 23 ppbv, whereas it is 11 ppbv for the polluted data subset. There is, however, a small population from that subset (21 occurrences spanning 12 summer days) that have background concentrations above 30 ppbv and total surface O_3 above 80 ppbv. This population increases to 59 occurrences spanning 26 summer days if we consider background concentrations above 25 ppbv. Further analysis reveals that these values occur on days with convective precipitation, which is associated with subsidence from above that transports background O_3 down to the surface. Alongside the subgrid-scale convective activity in the model, there is enough photochemical production of O_3 in the mixed layer to sustain elevated levels of surface O_3. This finding reveals that conditions do exist under which the background O_3 can contribute substantially to total surface concentrations above 80 ppbv. However, some of the background transported convectively to the surface may have been produced from North American anthropogenic precursors previously lofted to the free troposphere. Further

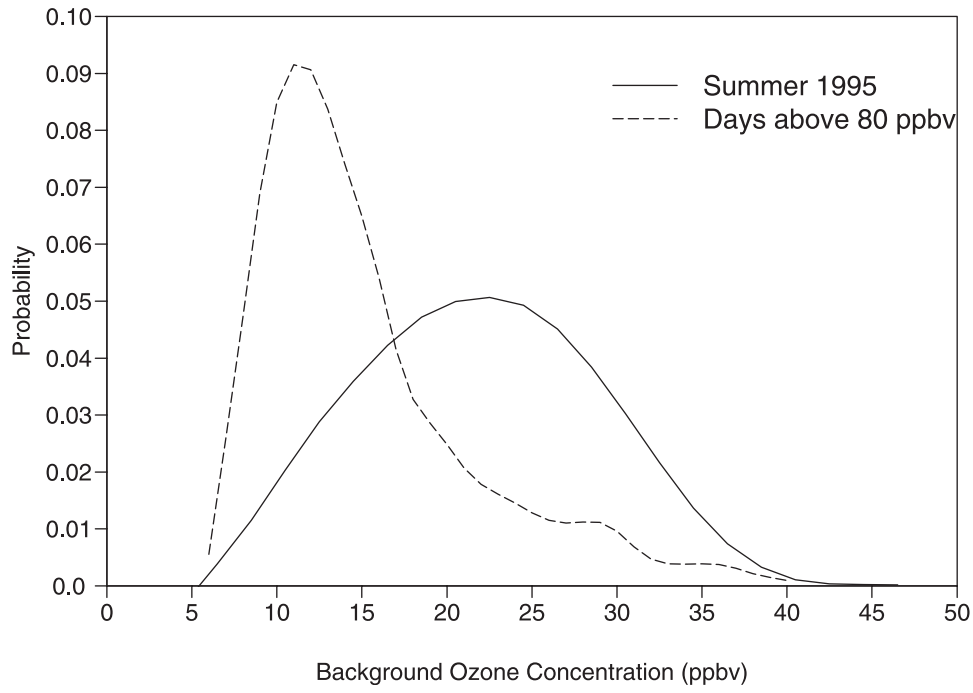

Figure 12. Probability distribution of summer afternoon background O_3 concentrations over the United States in the model surface air for the ensemble of data for summer 1995 (solid line) and for those days when surface O_3 exceeded 80 ppbv (dotted line). The background is defined as O_3 produced outside the North American boundary layer (surface to 700 hPa).

analysis of the origin of the background is presented in the next section.

6. Origin of the Background

[51] Because of chemical nonlinearity, the background O_3 defined by the tagged tracer simulation cannot be quantitatively related to precursor emissions; sensitivity simulations with modified emissions are necessary. In this section, we use a series of sensitivity simulations to quantify (1) the natural background and (2) the enhancement to the background from anthropogenic emissions outside of North America.

[52] We conducted three sensitivity studies in the coarser resolution ($4° \times 5°$) model in which we removed all anthropogenic emissions of NO_x, CO, and nonmethane hydrocarbons (including NO_x emitted from aircraft and fertilizer, but not biomass burning): (1) globally, (2) within North America, and (3) only outside of North America. Natural sources of NO_x from soil and lightning remain. We consider biomass burning as a natural source because of the lack of information on trends in biomass burning over the past century. Anthropogenic biomass burning is minimal during the summer months in the Northern Hemisphere, with episodic boreal fires (over two thirds of which are ignited naturally by lightning [*Stocks*, 1991]) predominantly responsible for biomass burning emissions (Duncan et al., submitted manuscript, 2002).

[53] We define the North American domain to be north of 12°N latitude and between 62.5°W and 127.5°W longitude. All sensitivity simulations are initialized for a full year from 1 June 1994 through 31 May 1995 and results from 1 June to 31 August 1995 are examined. One year provides sufficient initialization to remove the effects of initial O_3 concentrations on the results.

[54] Sensitivity simulation 1 serves to isolate a "natural" background. Figure 13a displays the resulting distribution of O_3 in surface air over the United States in summer. The corresponding spatial concentration statistics are shown in Table 3. The average afternoon (1300–1700 LT) concentration from June–August is 25 ppbv (compared to 51 ppbv in the standard simulation), with a spatial variance of 10 $ppbv^2$ (72 $ppbv^2$ in the standard simulation). Similar to the results from our tagged tracer study, we find the natural background to be highest in the arid southwestern United States. In comparison to the results presented here, preindustrial model simulations show surface O_3 concentrations over the United States of 10–20 ppbv; these lower values reflect the effect of lower concentrations of preindustrial methane, and the use of 24-hour average values as compared to the afternoon values we present here [*Wang and Jacob*, 1998; *Mickley et al.*, 1999; *Lelieveld and Dentener*, 2000].

[55] Figure 13b shows results from sensitivity simulation 2 which includes anthropogenic emissions only outside of North America. The mean summer afternoon O_3 concentration in the model surface layer over the United States is 30 ppbv, with a spatial variance of 12 $ppbv^2$ (Table 3). Figure 13c shows the difference between simulations 2 and 1, which represents the enhancement in the O_3 background in the United States due to anthropogenic emissions outside North America (i.e., from Asia and Europe). We find that this enhancement to summer afternoon O_3 concentrations is 4–7 ppbv on average and is largest in the west.

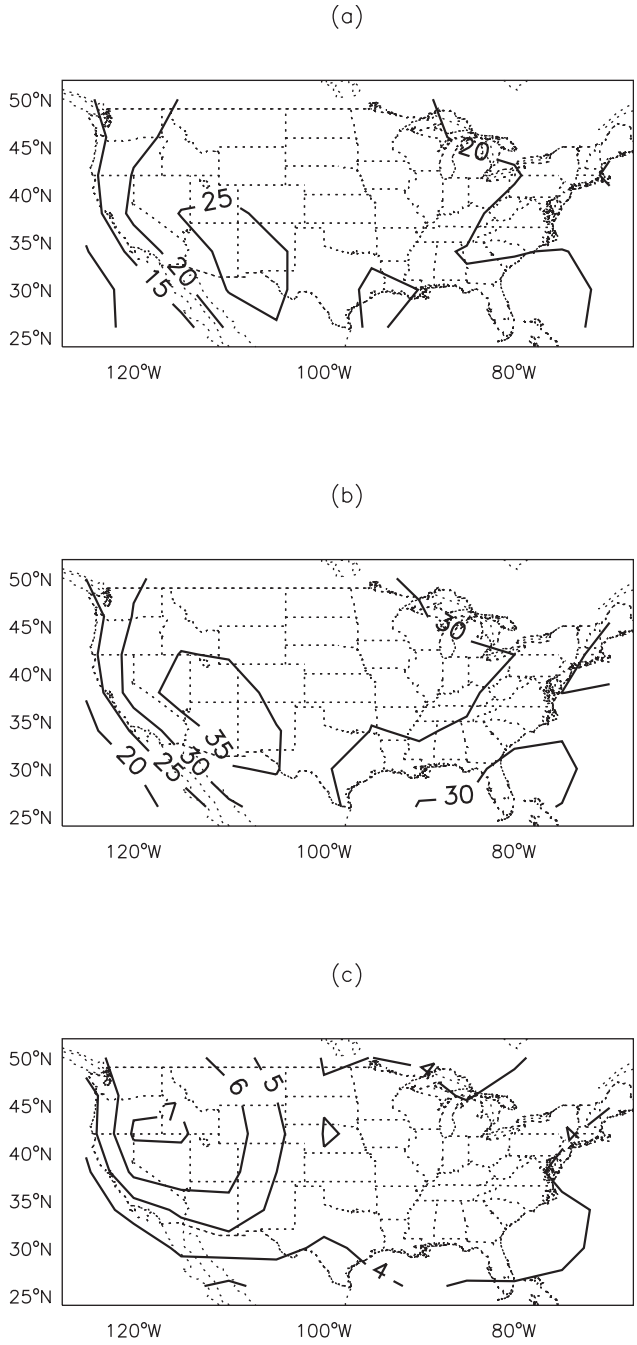

Figure 13. Background concentrations of O_3 in the summer of 1995, as obtained in sensitivity simulations with modified emissions. Values are afternoon (1300–1700 LT) averages in surface air in June–August. (a) Natural background, with all anthropogenic emissions of NO_x, CO, and nonmethane hydrocarbons turned off. (b) Non-U.S. background, with anthropogenic emissions in North America turned off. (c) Difference between the two, representing the enhancement of O_3 in surface air over the United States resulting from anthropogenic emissions outside of North America (i.e., Asia and Europe).

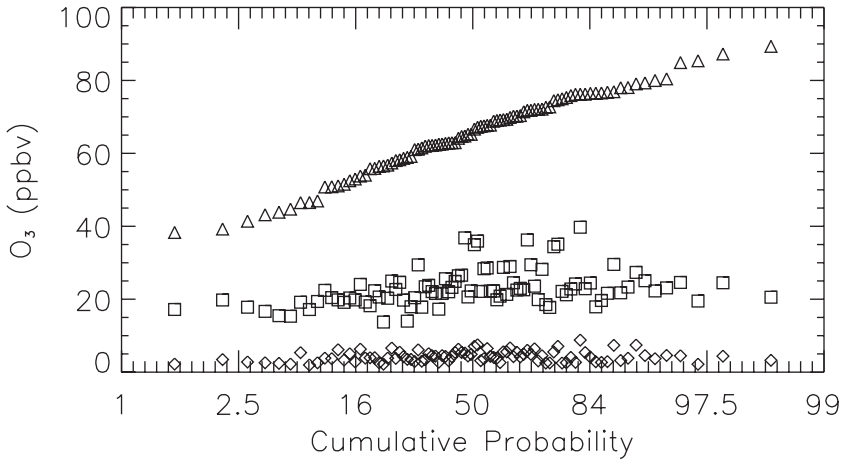

Figure 14. Cumulative probability distribution of simulated afternoon O_3 concentrations in the model surface air at Harvard Forest, Massachusetts (triangles). The corresponding contributions from the natural background are shown as squares (sensitivity simulation 1) and the anthropogenic enhancement due to emissions in Asia and Europe is shown as diamonds (difference between sensitivity simulations 2 and 1).

[56] Figure 14 displays the results of the sensitivity simulations in terms of the frequency distribution of surface afternoon O_3 in the standard simulation at Harvard Forest (open triangles). The natural background as defined by sensitivity simulation 1 (open squares) does not exhibit the decrease with higher O_3 that was found in the tagged tracer simulation discussed in section 5 (solid triangles in Figure 6). The tagged tracer simulation did not account for O_3 production from natural precursors in the North American boundary layer, which compensates for decreased transport from the free troposphere during stagnation events. The impact of anthropogenic emissions outside North America (open diamonds in Figure 14) is 2–9 ppbv over the range of conditions encountered at Harvard Forest in the model, and tends to be highest for O_3 concentrations in the range 55–75 ppbv.

[57] In Figure 15, we examine the O_3 enhancement from Asian and European emissions for the entire population of summer afternoon O_3 concentrations over the United States in the model surface layer. The decrease in this enhancement for the highest O_3 concentrations (>80 ppbv) is consistent with our finding in section 5; the lifetime of O_3 is short enough that the background is depleted under the stagnant conditions associated with high-O_3 episodes. Even so, Asian and European emissions enhance summer afternoon O_3 levels in surface air by 2–7 ppbv under these episodic conditions. The low tail of the O_3 frequency distribution (below 40 ppbv) is associated with only small

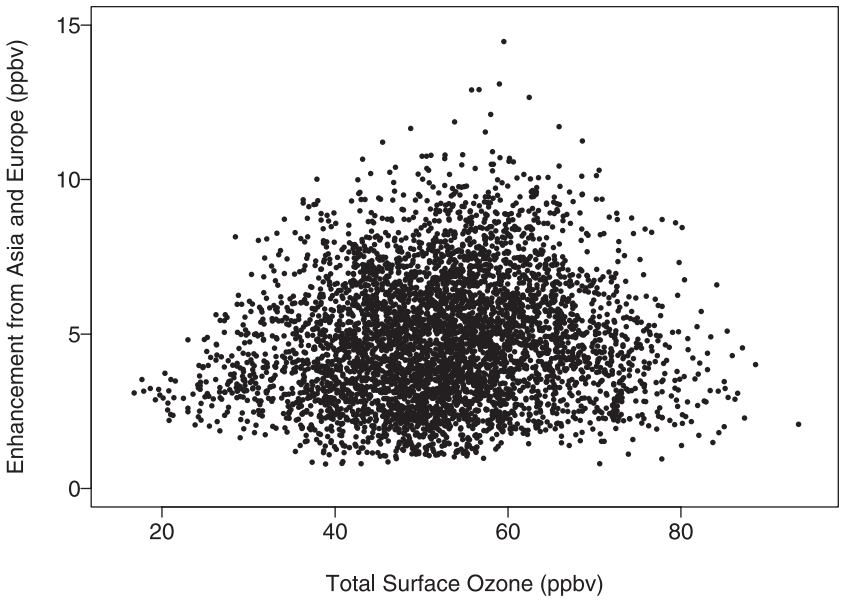

Figure 15. Enhancement to afternoon background O_3 in surface air over the United States due to anthropogenic emissions in Asia and Europe, plotted as a function of total O_3 concentrations in the model surface layer. Points represent daily afternoon (1300–1700 LT) model values for the ensemble of days in June–August 1995 for all U.S. grid squares.

enhancements from emissions outside of North America. We attribute these clean values to boundary layer transport of air masses originating from the tropics or the Arctic, with minimal impact from Asian and European emissions. Generalizing from the results at Harvard Forest (Figure 14), we observe in Figure 15 a maximum influence of Asian and European emissions (up to 14 ppbv) for concentrations of 50–70 ppbv. These conditions reflect a combination of subsidence of O_3 from the free troposphere (often associated with convective precipitation events) and fast photochemical production of O_3 in the U.S. boundary layer, as discussed in section 5; the present analysis allows us to quantify the exogenous pollution component of this subsiding background. Our result implies that if a more stringent national O_3 standard were to be adopted in the United States (such as the 60 ppbv standard in Japan and many European nations), it would be essential to consider the major role played by Asian and European anthropogenic emissions in exceedances of the standard.

[58] Sensitivity simulation 3, with anthropogenic emissions only within North America, was conducted to explore how chemical non-linearities may affect our estimate of the impact of foreign emissions on domestic air quality (Figure 13c). This simulation yields a mean summer afternoon surface O_3 of 46 ppbv, which is 5 ppbv less than the value from the standard simulation (Table 3). The difference between the standard simulation and simulation (3) enables us to make a second estimate of the impact of anthropogenic emissions from outside North America on surface background concentrations in the United States. We find the range of influence derived from this approach to be consistent with our previous approach: 4–7 ppbv, with a similar spatial distribution. The difference between sensitivity simulations 1 and 2 on the one hand, and between the standard simulation and sensitivity simulation 3 on the other hand, allows us to bracket the effect of chemical nonlinearity in terms of quantifying the O_3 enhancement over North America due to anthropogenic emissions from outside. We find that the effect of nonlinearity is less than 1 ppbv.

7. Conclusions

[59] We have applied a three–dimensional global model of tropospheric chemistry driven by assimilated meteorological observations for 1995 to identify the origin of background O_3 in surface air over the United States on summer (June through August) afternoons (1300–1700 LT). A tagged tracer simulation enabled us to quantify the contribution to O_3 from chemical production outside the North American boundary layer, and to examine the importance of the background on both average and highly polluted days. Sensitivity simulations were employed to quantify the natural component of this background and the enhancement from emissions outside of North America (from Asia and Europe).

[60] Extensive evaluation of model results with 1995 observations from several networks was conducted to assess the ability of the model to simulate regional chemistry over the United States under the range of conditions from relatively clean to highly polluted. Comparison with surface and aircraft measurements from the summer of 1995 indicates that the GEOS-CHEM model reproduces much of the observed variability in the summertime afternoon O_3 distribution, including the observed high-O_3 events. Consistent with previous analyses of O_3 observations in surface air over the United States [*Lefohn et al.*, 1998; *Lin et al.*, 2000], we find that a comparison of simulations with 1995 versus 1980 global fossil fuel emissions reveals a decrease in the high end of the O_3 probability distribution (due to domestic hydrocarbon emission controls) and an increase in the lower half of the distribution (from rising Asian emissions). The most severe limitation for our study is the inability of the model to capture background levels of O_3 on clean days in the southeastern United States. This problem arises from excessive convection over the Gulf of Mexico and the Caribbean, which mixes down too much O_3 from aloft.

[61] With our tagged O_3 tracer simulation, we find that chemical production outside of the North American boundary layer (surface - 700 hPa) contributes an average 15–35 ppbv background to summertime afternoon O_3 in surface air over the United States. This background is mainly produced in the free troposphere. Contribution from the stratosphere is negligible (less than 2 ppbv). The background is higher in the western than in the eastern United States, reflecting the longer O_3 lifetime in the west. We find that the lifetime of O_3 (actually the extended odd oxygen family) in the mixed layer over the eastern United States is only about 2 days because of shallow mixing depths, relatively high deposition velocities, and significant contributions to O_3 loss from reactions with biogenic hydrocarbons and HNO_3 deposition. Because of this short lifetime, background O_3 concentrations in the east generally drop to below 12 ppbv during high-O_3 episodes associated with regional stagnation. Consequently, an estimate of the background O_3 contribution based on observations under clean conditions severely overestimates the actual background under the heavily polluted conditions associated with exceedances of the national air quality standard.

[62] We find that in 3% of events where O_3 exceeds 80 ppbv in the model, background O_3 transported from outside the North American boundary layer contributes 30–40 ppbv. In 9% of all such events, background O_3 contributes above 25 ppbv. These events are associated with deep convection upstream that entrain background O_3 from the free troposphere, followed by rapid production of additional O_3 within the U.S. boundary layer.

[63] Our sensitivity simulations show that anthropogenic emissions from Asia and Europe enhance afternoon O_3 in surface air over the United States in summer afternoons by 4–7 ppbv on average. This enhancement is maximum for O_3 concentrations in the 50–70 ppbv range when subsidence from the free troposphere associated with convection events combines with subsequent O_3 production in the U.S. boundary layer. The enhancement from these exogenous anthropogenic emissions is less (2–7 ppbv) under the heavily polluted conditions leading to exceedances of the 80 ppbv threshold. Nevertheless, it is important to consider this relatively small influence of Asian and European emissions in the context of the substantially less-than-linear response of O_3 to domestic emission controls [*Liang et al.*, 1998; *Jacob et al. 1999*; *Sillman*, 1999; *Ryerson et al.*, 2001]. If emissions from developing countries follow their projected increasing trends [*Prather and Ehhalt*, 2001], we

can expect this contribution to rise in future years. Furthermore, if the O_3 standard in the United States is lowered to below 70 ppbv in the future (as it already is in many nations, to protect vegetation as well as human health), then consideration of the large enhancement from anthropogenic emissions outside North America will become an essential element in the development of an emission control strategy.

[64] **Acknowledgments.** This research was supported by the Electric Power Research Institute (EPRI), by the NASA Atmospheric Chemistry Modeling and Analysis Program (ACMAP) and by an NSF Graduate Study Fellowship to A. Fiore. The authors are grateful to M. Gupta (EPRI), S. McKeen, and D. Parrish for useful discussions and to B. Doddridge, G. Hubler, S. McKeen, B. Norris, K. Schere, and B. Wittig for providing data from SOS and NARSTO-NE.

References

Allen, D. J., R. B. Rood, A. M. Thompson, and R. D. Hudson, Three-dimensional radon 222 calculations using assimilated meteorological data and a convective mixing algorithm, *J. Geophys. Res.*, *101*, 6871–6881, 1996.

Allen, D. J., K. E. Pickering, and A. Molod, An evaluation of deep convective mixing in the Goddard Chemical Transport Model using International Satellite Cloud Climatology Project cloud parameters, *J. Geophys. Res.*, *102*, 25,467–25,476, 1997.

Altshuller, A. P., and A. S. Lefohn, Background ozone in the planetary boundary layer over the United States, *J. Air Waste Manage. Assoc.*, *46*, 134–141, 1996.

Anderson, J. A., B. M. Schoell, and D. B. Wright, Selected NARSTO-Northeast aircraft data for July 31, 1995, *EPRI TR-109532*, Electr. Power Res. Inst., Palo Alto, Calif., 1996.

Anfossi, D., S. Sandroni, and S. Viarengo, Tropospheric ozone in the nineteenth century: The Moncalieri Series, *J. Geophys. Res.*, *96*, 17,349–17,352, 1991.

Banta, R. M., et al., Daytime buildup and nighttime transport of urban ozone in the boundary layer during a stagnation episode, *J. Geophys. Res.*, *103*, 22,519–22,544, 1998.

Beck, J. P., and P. Grennfelt, Estimate of ozone production and destruction over northwestern Europe, *Atmos. Environ.*, *28*, 129–140, 1994.

Bell, N., L. Hsu, D. J. Jacob, M. G. Schultz, D. R. Blake, J. Butler, and E. Maier-Reimer, Global budgets of oceanic and atmospheric methyl iodide: Development of methyl iodide as a tracer for marine convection in atmospheric models, *J. Geophys. Res.*, 2002.

Benkovitz, C. M., M. T. Schultz, J. Pacyna, L. Tarrason, J. Dignon, E. C. Voldner, P. A. Spiro, J. A. Logan, and T. E. Graedel, Global gridded inventories for anthropogenic emissions of sulfur and nitrogen, *J. Geophys. Res.*, *101*, 29,239–29,253, 1996.

Berman, S., J. Y. Ku, and S. T. Rao, Spatial and temporal variation in the mixing depth over the northeastern United States during the summer of 1995, *J. Appl. Meteorol.*, *38*, 1661–1673, 1999.

Bey, I., D. J. Jacob, R. M. Yantosca, J. A. Logan, B. D. Field, A. M. Fiore, Q. Li, H. Y. Liu, L. J. Mickley, and M. Schultz, Global modeling of tropospheric chemistry with assimilated meteorology: Model description and evaluation, *J. Geophys. Res.*, *106*, 23,073–23,096, 2001a.

Bey, I., D. J. Jacob, J. A. Logan, and R. M. Yantosca, Asian chemical outflow to the Pacific: Origins, pathways, and budgets, *J. Geophys. Res.*, *106*, 23,097–23,114, 2001b.

Blumenthal, D. L., F. W. Lurmann, N. Kumar, T. S. Dye, S. E. Ray, M. Korc, R. Londergan, and G. Moore, *NARSTO- Northeast Transport and Mixing Phenomena Related to Ozone Exceedances in the Northeast United States*, draft version 1.0, Sonoma Technology, Inc., Santa Rosa, Calif., 1997.

Chen, X., D. Hulbert, and P. B. Shepson, Measurement of the organic nitrate yield from OH reaction with isoprene, *J. Geophys. Res.*, *103*, 25,563–25,568, 1998.

Chin, M., D. J. Jacob, G. M. Gardner, M. S. Foreman-Fowler, P. A. Spiro, and D. L. Savoie, A global three-dimensional model of tropospheric sulfate, *J.Geophys. Res.*, *101*, 18,667–18,690, 1996.

Cowling, E. B., W. L. Chameides, C. S. Kiang, F. C. Fehsenfeld, and J. F. Meagher, Introduction to the special section: Southern Oxidants Study Nashville/Middle Tennessee Ozone Study, *J. Geophys. Res.*, *103*, 22,209–22,212, 1998.

Cowling, E. B., W. L. Chameides, C. S. Kiang, F. C. Fehsenfeld, and J. F. Meagher, Introduction to special section: Southern Oxidants Study Nashville/Middle Tennessee Ozone Study, Part 2, *J. Geophys. Res.*, *105*, 9075–9077, 2000.

Dickerson, R., S. Kondragunta, G. Stenchikov, K. Civerolo, B. Doddridge, and B. Holben, The impact of aerosols on solar ultraviolet radiation and photochemical smog, *Science*, *278*, 827–830, 1997.

Duncan, B. N., and J. A. Logan, Trends in carbon monoxide (1988–1997): A model sensitivity study, *Eos Trans. AGU*, *82*(20), Spring Meet. Suppl., A62B-06, 2001.

E. H. Pechan and Associates, Inc., Development of SAMI 1990 Base Year Emissions Inventory, draft report prepared for Southern Appalachian Mountains Initiative, Springfield, Va., January 1999.

Environmental Protection Agency, National air pollutant emission trends, 1990–1996, *EPA-454/R-97-011*, Research Triangle Park, N. C., 1997.

Environmental Protection Agency, National air quality and emissions trends report: 1998, *EPA-454/R-00-003*, Research Triangle Park, N. C., 2000. (Available at www.epa.gov/airs/criteria.html)

Environmental Protection Agency, National air quality and emissions trends report: 1999, *EPA-454/R-01-004*, Research Triangle Park, N. C., 2001. (Available at http://www.epa.gov/oar/aqtrnd99/toc.html)

Follows, M. J., and J. F. Austin, A zonal average model of the stratospheric contributions to the tropospheric ozone budget, *J. Geophys. Res.*, *97*, 18,047–18,060, 1992.

Goldan, P. D., D. D. Parrish, W. C. Kuster, M. Trainer, S. A. McKeen, J. Holloway, B. T. Jobson, D. T. Sueper, and F. C. Fehsenfeld, Airborne measurements of isoprene, CO, and anthropogenic hydrocarbons and their implications, *J. Geophys. Res.*, *105*, 9091–9105, 2000.

Guenther, A., et al., A global model of natural volatile organic compound emissions, *J. Geophys. Res.*, *100*, 8873–8892, 1995.

Hallock-Waters, K. A., B. G. Doddridge, R. R. Dickerson, S. Spitzer, and J. D. Ray, Carbon monoxide in the U.S. mid-Atlantic troposphere: Evidence for a decreasing trend, *Geophys. Res. Lett.*, *26*, 2861–2864, 1999.

Hauglustaine, D. A., G. P. Brasseur, S. Walters, P. J. Rasch, J.-F. Muller, L. K. Emmons, and M. A. Carroll, MOZART, a global chemical transport model for ozone and related chemical tracers, 2, Model results and evaluation, *J. Geophys. Res.*, *103*, 28,291–28,335, 1998.

Herman, J. R., and E. A. Celarier, Earth surface reflectivity climatology at 340–380 nm from TOMS data, *J. Geophys. Res.*, *102*, 28,003–28,011, 1997.

Hirsch, A. I., J. W. Munger, D. J. Jacob, L. W. Horowitz, and A. H. Goldstein, Seasonal variation of the ozone production efficiency per unit NO_x at Harvard Forest, Massachusetts, *J. Geophys. Res.*, *101*, 12,659–12,666, 1996.

Hirsch, R. M., and E. J. Gilroy, Methods of fitting a straight line to data: Examples in water resources, *Water Res. Bull.*, *20*, 705–711, 1984.

Holzworth, G. C., Mixing depths, wind speeds and air pollution potential for selected locations in the United States, *J. Appl. Meteorol.*, *6*, 1039–1044, 1967.

Horowitz, L. W., J. Liang, G. M. Gardner, and D. J. and Jacob, Export of reactive nitrogen from North America during summertime, *J. Geophys. Res.*, *103*, 13,451–13,476, 1998.

Hubler, G., et al., An overview of the airborne activities during the Southern Oxidants Study (SOS) 1995 Nashville/Middle Tennessee Ozone Study, *J. Geophys. Res.*, *103*, 22,245–22,259, 1998.

Jacob, D. J., Heterogeneous chemistry and tropospheric ozone, *Atmos. Environ.*, *34*, 2131–2159, 2000.

Jacob, D. J., et al., Summertime photochemistry of the troposphere at high northern latitudes, *J. Geophys. Res.*, *97*, 16,421–16,431, 1992.

Jacob, D. J., et al., Simulation of summertime ozone over North America, *J. Geophys. Res.*, *98*, 14,797–14,816, 1993a.

Jacob, D. J., J. A. Logan, G. M. Gardner, R. M. Yevich, C. M. Spivakovsky, and S. C. Wofsy, Factors regulating ozone over the United States and its export to the global atmosphere, *J. Geophys. Res.*, *98*, 14,817–14,826, 1993b.

Jacob, D. J., J. A. Logan, and P. P. Murti, Effect of rising Asian emissions on surface ozone in the United States, *Geophys. Res. Lett.*, *26*, 2175–2178, 1999.

Jacob, D. J., B. D. Field, E. Jin, I. Bey, Q. Li, J. A. Logan, R. M. Yantosca, and H. B. Singh, Atmospheric budget of acetone, *J. Geophys. Res.*, *107*, 10.1029/2001JD000694, 2002.

Jacobson, M. Z., and R. P. Turco, A sparse-matrix, vectorized GEAR code for atmospheric transport models, *Atmos. Environ.*, *33*, 273–284, 1994.

Kasibhatla, P., H. Levy II, A. Klonecki, and W. L. Chameides, Three-dimensional view of the large-scale tropospheric ozone distribution over the North Atlantic Ocean during summer, *J. Geophys. Res.*, *101*, 29,305–29,316, 1996.

Kasibhatla, P., W. L. Chameides, R. D. Saylor, and D. Olerud, Relationships between regional ozone pollution and emissions of nitrogen oxides in the eastern United States, *J. Geophys. Res.*, *103*, 22,663–22,669, 1998.

Kondragunta, S., The impact of aerosols on urban photochemical smog production, Ph.D. thesis, Univ. of Md., College Park, 1997.

Korc, M., P. Roberts, and D. Blumenthal, NARSTO-Northeast Data Management Plan, *EPRI TR-109541*, Sonoma Technology, Inc., Santa Rosa, Calif., 1996.

Lavery, T. F., C. M. Rogers, M. O. Stewart, H. K. Howell, C. M. Costakis, M. C. Burnett, W. R. Barnard, and C. A. Wanta, The U.S. Environmental Protection Agency (EPA) Clean Air Status and Trends Network (CASTNet) 1999 annual report, prepared by Environmental Science and Engineering, Inc., for U.S. EPA Office of Air Quality Planning and Standards, *EPA contract 68-D-98-112*, Research Triangle Park, N. C., 2001.

Lawrence, M. G., P. J. Crutzen, P. J. Rasch, B. E. Eaton, and N. M. Mahowald, A model for studies of tropospheric photochemistry: Description, global distributions, and evaluation, *J. Geophys. Res.*, *104*, 26,245–26,277, 1999.

Lefohn, A. S., D. S. Shadwick, and S. D. Ziman, The difficult challenge of attaining EPA's new ozone standard, *Environ. Sci. Technol.*, *32*, 276A–282A, 1998.

Lefohn, A. S., S. J. Oltmans, T. Dann, and H. B. Singh, Present-day variability of background ozone in the lower troposphere, *J. Geophys. Res.*, *106*, 9945–9958, 2001.

Lelieveld, J., and F. J. Dentener, What controls tropospheric ozone?, *J. Geophys. Res.*, *105*, 3531–3551, 2000.

Li, Q., D. J. Jacob, I. Bey, R. M. Yantosca, Y. Zhao, Y. Kondo, and J. Notholt, Atmospheric hydrogen cyanide (HCN): Biomass burning source, ocean sink?, *Geophys. Res. Lett.*, *27*, 357–360, 2000.

Li, Q., et al., A tropospheric ozone maximum over the Middle East, *Geophys. Res. Lett.*, *28*, 3235–3238, 2001.

Li, Q., D. J. Jacob, T. D. Fairlie, H. Liu, R. M. Yantosca, and R. V. Martin, Stratospheric versus pollution influences on ozone at Bermuda: Reconciling past analyses, *J. Geophys. Res.*, *107*, 10.1029/2002JD002138, in press, 2002.

Liang, J., and M. Z. Jacobson, Effects of subgrid segregation on ozone production efficiency in a chemical model, *Atmos. Environ.*, *34*, 2975–2982, 2000.

Liang, J., L. W. Horowitz, D. J. Jacob, Y. Wang, A. M. Fiore, J. A. Logan, G. M. Gardner, and J. W. Munger, Seasonal variations of reactive nitrogen species and ozone over the United States, and export fluxes to the global atmosphere, *J. Geophys. Res.*, *103*, 13,435–13,450, 1998.

Lin, C. Y., D. J. Jacob, J. W. Munger, and A. M. Fiore, Increasing background ozone in surface air over the United States, *Geophys. Res. Lett.*, *27*, 3465–3468, 2000.

Liu, H., D. J. Jacob, I. Bey, and R. M. Yantosca, Constraints from ^{210}Pb and ^{7}Be on wet deposition and transport in a global three-dimensional chemical tracer model driven by assimilated meteorological fields, *J. Geophys. Res.*, *106*, 12,109–12,128, 2001.

Liu, H., D. J. Jacob, L. Y. Chan, S. J. Oltmans, R. M. Yantosca, J. M. Harris, B. N. Duncan, and R. V. Martin, Sources of tropospheric ozone along the Asian Pacific Rim: An analysis of ozonesonde observations, *J. Geophys. Res.*, *107*, 10.1029/2001JD002005, in press, 2002.

Logan, J. A., Ozone in rural areas of the United States, *J. Geophys. Res.*, *94*, 8511–8532, 1989.

Logan, J. A., et al., Trends in the vertical distribution of ozone: A comparison of two analyses of ozonesonde data, *J. Geophys. Res.*, *104*, 26,373–26,399, 1999.

Luke, W. T., T. B. Watson, K. J. Olszyna, R. L. Gunter, R. T. McMillen, D. L. Wellman, and S. W. Wilkison, A comparison of airborne and surface trace gas measurements during the Southern Oxidants Study (SOS), *J. Geophys. Res.*, *103*, 22,317–22,337, 1998.

Marenco, A., H. Gouget, P. Nedelec, J. P. Pages, and F. Karcher, Evidence of a long-term increase in tropospheric ozone from Pic du Midi data series: Consequences: Positive radiative forcing, *J. Geophys. Res.*, *99*, 16,617–16,632, 1994.

Martin, R. V., et al., An improved retrieval of tropospheric nitrogen dioxide from GOME, *J. Geophys.*, *107*, 10.1029/2001JD001027, in press, 2002.

McKeen, S. A., G. Wotawa, M. Trainer, E. Hsie, D. D. Parrish, J. Holloway, and T. Ryerson, Ozine production from Canadian wildfires during the 1995 Southern Oxidant Study, *Eos Trans. AGU*, *81*(48), Fall Meet. Suppl., A11B-40, 2000.

McKeen, S. A., G. Wotawa, D. D. Parrish, J. S. Holloway, M. P. Buhr, G. Hubler, F. C. Fehsenfeld, and J. F. Meagher, Ozone production from Canadian wildfires during June and July of 1995, *J. Geophys. Res.*, *107*, 10.1029/2001JD000697, in press, 2001.

McLinden, C. A., S. C. Olsen, B. Hannegan, O. Wild, M. J. Prather, and J. Sundet, Stratospheric ozone in 3-D models: A simple chemistry and the cross-tropopause flux, *J. Geophys. Res.*, *105*, 14,653–14,665, 2000.

McNider, R. T., W. B. Norris, A. J. Song, R. L. Clymer, S. Gupta, R. M. Banta, R. J. Zamora, A. B. White, and M. Trainer, Meteorological conditions during the 1995 Southern Oxidants Study Nashville/Middle Tennessee Field Intensive, *J. Geophys. Res.*, *103*, 22,225–22,243, 1998.

Meagher, J. F., E. B. Cowling, F. C. Fehsenfeld, and W. J. Parkhurst, Ozone formation and transport in the southeastern United States: Overview of the SOS Nashville/Middle Tennessee Ozone Study, *J. Geophys. Res.*, *103*, 22,213–22,223, 1998.

Mickley, L. J., P. P. Murti, D. J. Jacob, J. A. Logan, D. Rind, and D. Koch, Radiative forcing from tropospheric ozone calculated with a unified chemistry-climate model, *J. Geophys. Res.*, *104*, 30,153–30,172, 1999.

Mueller, P. K., P. Roberts, M. Korc, and D. Blumenthal, NARSTO-Northeast 1995 Summer Ozone Study, version 1.2, *EPRI TR-109540*, Electr. Power Res. Inst., Palo Alto, Calif., 1996.

Munger, J. W., S. C. Wofsy, P. S. Bakwin, S.-M. Fan, M. L. Goulden, B. C. Daube, A. H. Goldstein, K. E. Moore, and D. R. Fitzjarrald, Atmospheric deposition of reactive nitrogen oxides and ozone in a temperate deciduous forest and a sub-arctic woodland, 1, Measurements and mechanisms, *J. Geophys. Res.*, *101*, 12,639–12,657, 1996.

Munger, J. W., S.-M. Fan, P. S. Bakwin, M. L. Goulden, A. H. Goldstein, A. S. Colman, and S. C. Wofsy, Regional budgets for nitrogen oxides from continental sources: Variations of rates for oxidation and deposition with season and distance from source regions, *J. Geophys. Res.*, *103*, 8355–8368, 1998.

NARSTO Synthesis Team, An assessment of tropospheric ozone pollution: A North American perspective, draft report, Electr. Power Res. Inst., Palo Alto, Calif., July 2000.

National Research Council, *Rethinking the Ozone Problem in Urban and Regional Air Pollution*, Natl. Acad., Washington D. C., 1991.

Ogburn, C., L. Boothe, M. Mullen, and P. F. Brewer, Emissions inventories for the Southern Appalachian Mountains Initiative, paper presented at Annual Meeting, Air and Waste Manage. Assoc., Salt Lake City, Utah, June 2000.

Olszyna, K. J., E. M. Bailey, R. Simonaitis, and J. F. Meagher, O_3 and NO_y relationships at a rural site, *J. Geophys. Res.*, *99*, 14,557–14,563, 1994.

Olszyna, K. J., W. J. Parkhurst, and J. F. Meagher, Air chemistry during the 1995 SOS/Nashville intensive determined from level 2 network, *J. Geophys. Res.*, *103*, 31,143–31,153, 1998.

Oltmans, S. J., et al., Trends of ozone in the troposphere, *Geophys. Res. Lett.*, *25*, 139–142, 1998.

Orlando, J. J., B. Noziere, G. S. Tyndall, G. E. Orzechowska, S. E. Paulson, and Y. Rudich, Product studies of the OH- and ozone-initiated oxidation of some monoterpenes, *J. Geophys. Res.*, *105*, 11,561–11,572, 2000.

Palmer, P. I., D. J. Jacob, K. Chance, R. V. Martin, D. R. J. Spurr, T. P. Kurosu, I. Bey, R. Yantosca, A. Fiore, and Q. Li, Air mass factor formulation for spectroscopic measurements from satellites: Application to formaldehyde retrievals from GOME, *J. Geophys. Res.*, *106*, 14,539–14,550, 2001.

Park, R. J., G. L. Stenchikov, K. E. Pickering, R. R. Dickerson, D. J. Allen, and S. Kondragunta, Regional air pollution and its radiative forcings: Studies with a single-column chemical and radiation transport model, *J. Geophys. Res.*, *106*, 28,751–28,770, 2002.

Parrish, D. D., M. Trainer, D. Hereid, E. J. Williams, K. J. Olszyna, R. A. Harley, J. F. Meagher, and F. C. Fehsenfeld, Decadal change in carbon monoxide to nitrogen oxide ratio in U. S. vehicular emissions, *J. Geophys. Res.*, *107*, 10.1029/2001JD000720, 2002.

Piccot, S. D., J. J. Watson, and J. W. Jones, A global inventory of volatile organic compound emissions from anthropogenic sources, *J. Geophys. Res.*, *97*, 9897–9912, 1992.

Prather, M., and D. Ehhalt, Atmospheric chemistry and greenhouse gases, in *Climate Change: The Scientific Basis: The IPCC Working Group 1 Third Assessment Report*, Cambridge Univ. Press, New York, 2001.

Rasch, P. J., N. M. Mahowald, and B. E. Eaton, Representations of transport, convection, and the hydrologic cycle in chemical transport models: Implications for the modeling of short-lived and soluble species, *J. Geophys. Res.*, *102*, 28,127–28,138, 1997.

Russell, P. B., P. V. Hobbs, and L. L. Stowe, Aerosol properties and radiative effects in the United States east coast haze plume: An overview of the Tropospheric Aerosol Radiative Forcing Observational Experiment (TARFOX), *J. Geophys. Res.*, *104*, 2213–2222, 1999.

Ryan, W. F., B. G. Doddridge, R. R. Dickerson, R. M. Morales, K. A. Hallock, P. T. Roberts, D. L. Blumenthal, J. A. Anderson, and K. L. Civerolo, Pollutant transport during a regional O_3 episode in the mid-Atlantic states, *J. Air Waste Manage. Assoc.*, *48*, 786–797, 1998.

Ryerson, R. B., et al., Observations of ozone formation in power plant plumes and implications for ozone control strategies, *Science*, *292*, 719–723, 2001.

Saylor, R. D., W. L. Chameides, and E. B. Cowling, Implications of the new ozone National Ambient Air Quality Standards for compliance in rural areas, *J. Geophys. Res.*, *103*, 31,137–31,141, 1998.

Seaman, N. L., and S. A. Michelson, Mesoscale meteorological structure of a high-ozone episode during the 1995 NARSTO-Northeast Study, *J. Appl. Meteorol.*, *39*, 384–398, 2000.

Sillman, S., The relation between ozone, NO_x and hydrocarbons in urban and polluted rural environments, *Atmos. Environ.*, *33*, 1821–1845, 1999.

St. John, J. C., W. L. Chameides, and R. Saylor, Role of anthropogenic NO_x and VOC as ozone precursors: A case study from the SOS Nashville/Middle Tennessee Ozone Study, *J. Geophys. Res.*, *103*, 22,415–22,423, 1998.

Stocks, B. J., The extent and impact of forest fires in northern circumpolar countries, in *Global Biomass Burning*, edited by J. S. Levine, pp. 197–202, MIT Press, Cambridge, Mass., 1991.

Trainer, M., E. J. Williams, D. D. Parrish, M. P. Buhr, E. J. Allwine, H. H. Westberg, F. C. Fehsenfeld, and S. C. Liu, Models and observations of the impact of natural hydrocarbons on rural ozone, *Nature*, *329*, 705–707, 1987.

Trainer, M., et al., Correlation of ozone with NO_y in photochemically aged air, *J. Geophys. Res.*, *98*, 2917–2925, 1993.

Vukovich, F. M., Regional-scale boundary layer ozone variations in the eastern United States and their association with meteorological variations, *Atmos. Environ.*, *29*, 2259–2273, 1995.

Wang, Y., and D. J. Jacob, Anthropogenic forcing on tropospheric ozone and OH since preindustrial times, *J. Geophys. Res.*, *103*, 31,123–31,135, 1998.

Wang, Y., D. J. Jacob, and J. A. Logan, Global simulation of tropospheric ozone-NO_x-hydrocarbon chemistry, 1, Model formulation, *J. Geophys. Res.*, *103*, 10,713–10,726, 1998a.

Wang, Y., D. J. Jacob, and J. A. Logan, Global simulation of tropospheric ozone-NO_x-hydrocarbon chemistry, 2, Model evaluation and global ozone budget, *J. Geophys. Res.*, *103*, 10,727–10,755, 1998b.

Wang, Y., D. J. Jacob, and J. A. Logan, Global simulation of tropospheric ozone-NO_x-hydrocarbon chemistry, 3, Origin of tropospheric ozone and effects of non-methane hydrocarbons, *J. Geophys. Res.*, *103*, 10,757–10,768, 1998c.

Wesely, M. L., Parameterization of surface resistances to gaseous dry deposition in regional-scale numerical models, *Atmos. Environ.*, *23*, 1293–1304, 1989.

Wild, O., X. Zhu, and M. Prather, Fast-J: Accurate simulation of in- and below-cloud photolysis in tropospheric chemistry models, *J. Atmos. Chem.*, *37*, 245–282, 2000.

Wotawa, G., and M. Trainer, The influence of Canadian forest fires on pollutant concentrations in the United States, *Science*, *288*, 324–328, 2000.

Zhang, J., and S. T. Rao, The role of vertical mixing in the temporal evolution of ground-level ozone concentrations, *J. Appl. Meteorol.*, *38*, 1674–1691, 1999.

Zhang, J., S. T. Rao, and S. M. Daggupaty, Meteorological processes and ozone exceedances in the northeastern United States during the 12–16 July 1995 episode, *J. Appl. Meteorol.*, *37*, 776–789, 1998.

I. Bey, Swiss Federal Institute of Technology, EPFL-ENAC-LMCA, CH-1015 Lausanne, Switzerland. (Isabelle.Bey@epfl.ch)

B. D. Field, A. M. Fiore, A. C. Fusco, D. J. Jacob, and R. M. Yantosca, Department of Earth and Planetary Sciences and Division of Engineering and Applied Sciences, Harvard University, 12 Oxford Street, Cambridge, MA 02138, USA. (bdf@io.harvard.edu; afiore@fas.harvard.edu; acf@io.harvard.edu; djj@io.harvard.edu; bmy@io.harvard.edu)

J. G. Wilkinson, School of Civil and Environmental Engineering, Georgia Institute of Technology, Atlanta, GA 30332, USA. (jwilkins@themis.ce.gatech.edu)

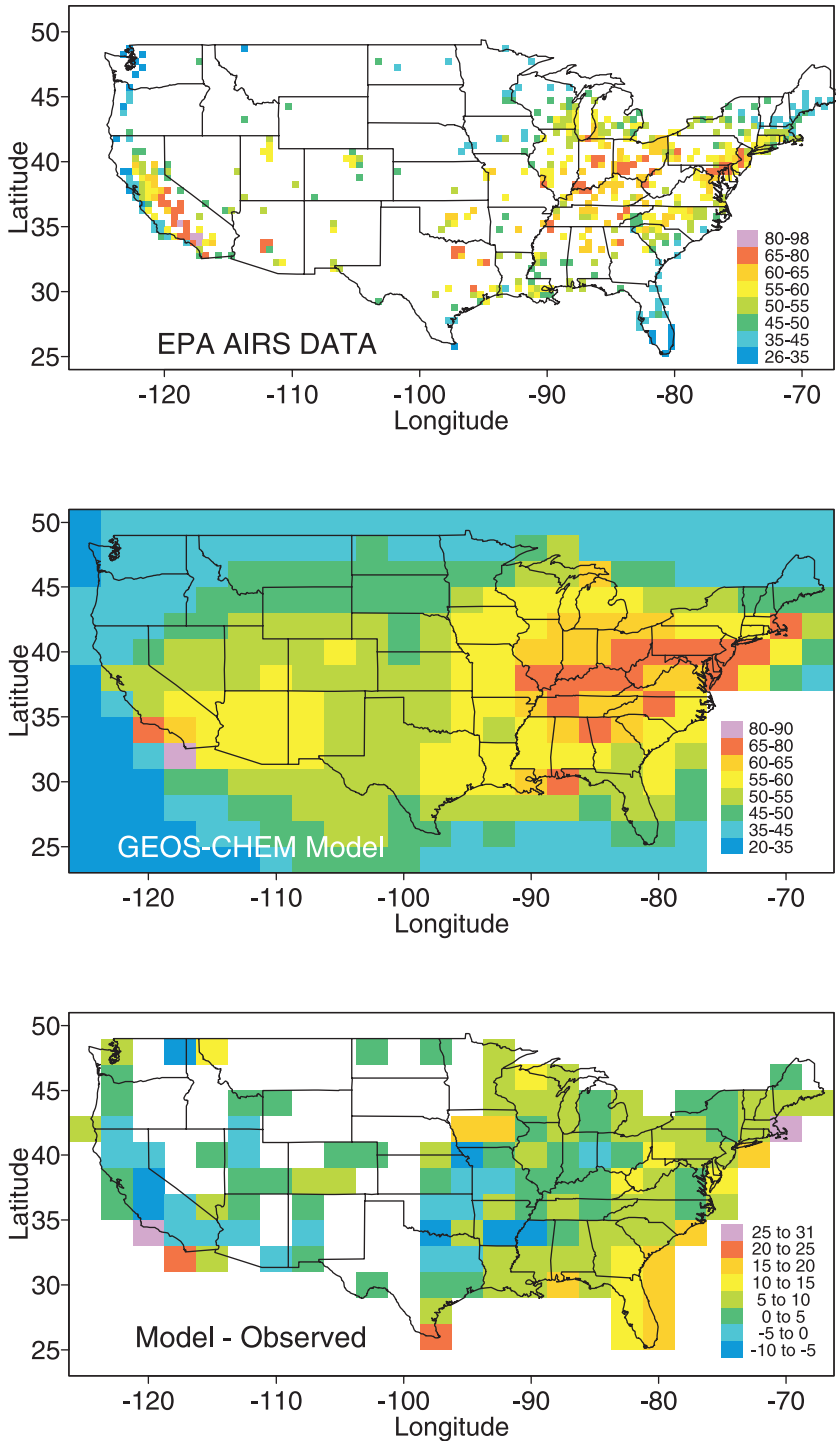

Figure 2. Average afternoon (1300–1700 LT) O_3 concentrations (ppbv) in surface air over the United States in June–August 1995 showing (top) the AIRS observations averaged over a 0.5° latitude by 0.5° longitude grid, (middle) results from the GEOS–CHEM model (2°– 2.5° resolution), sampled in the lowest model layer (0–100 m), and (bottom) the difference between model results and AIRS observations averaged over the 2° × 2.5° model grid.

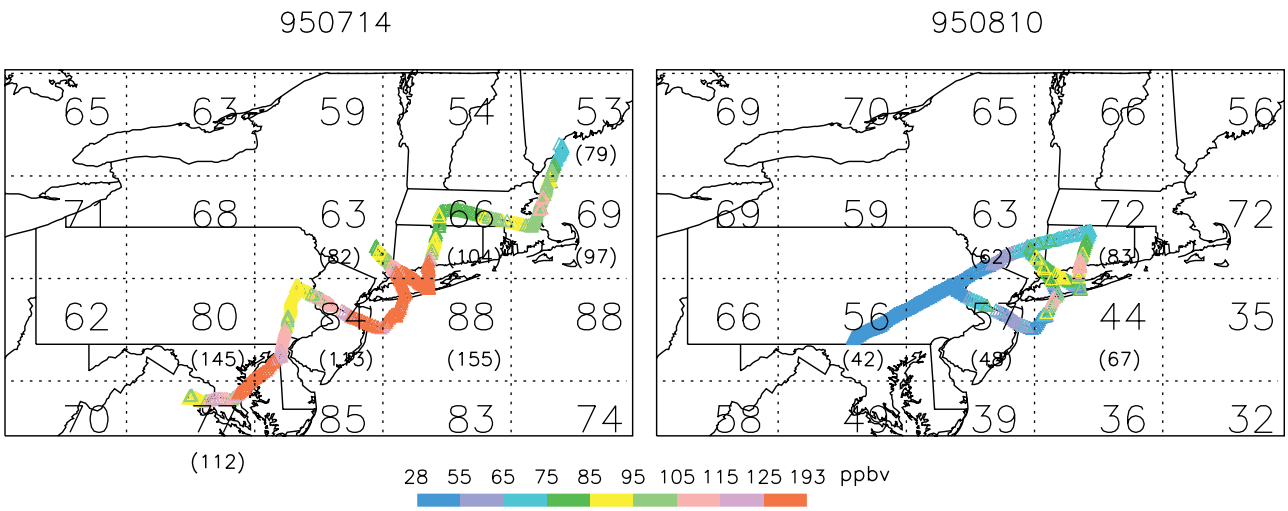

Figure 7. Ozone concentrations (ppbv) at 400–800 m altitude over the northeastern United States on 14 July and 10 August 1995. The lines show observations from the two NARSTO-NE aircraft. The model grid is superposed on each map, with the model O_3 concentration for that day (1300–1700 LT) printed at the center of each model box. Smaller numbers in parentheses are the average of all the aircraft data falling within each model grid box. We have selected days when both NARSTO-NE aircraft flew, providing the largest spatial coverage over the northeast region.